



HAL
open science

Modelling forest management within a global vegetation model-part 2: model validation from a tree to a continental scale

Valentin Bellassen, Gueric G. Le Maire, O. O. Guin, Jean-Francois Dhote Dhôte, Philippe Ciais, N. N. Viovy

► To cite this version:

Valentin Bellassen, Gueric G. Le Maire, O. O. Guin, Jean-Francois Dhote Dhôte, Philippe Ciais, et al.. Modelling forest management within a global vegetation model-part 2: model validation from a tree to a continental scale. *Ecological Modelling*, 2011, 222 (1), pp.57-75. 10.1016/j.ecolmodel.2010.08.038 . hal-01000729

HAL Id: hal-01000729

<https://hal.science/hal-01000729>

Submitted on 2 Jul 2021

HAL is a multi-disciplinary open access archive for the deposit and dissemination of scientific research documents, whether they are published or not. The documents may come from teaching and research institutions in France or abroad, or from public or private research centers.

L'archive ouverte pluridisciplinaire **HAL**, est destinée au dépôt et à la diffusion de documents scientifiques de niveau recherche, publiés ou non, émanant des établissements d'enseignement et de recherche français ou étrangers, des laboratoires publics ou privés.

1 **Title:** Modelling forest management within a global vegetation model – Part 2: model
2 validation from a tree to a continental scale

3

4 **Journal:** Ecological Modelling, Elsevier, 2011, 222 (1), pp.57-75.

5 <10.1016/j.ecolmodel.2010.08.038>

6 **Authors:** Bellassen V¹, le Maire G², Guin O¹, Dhôte JF³, Viovy N¹, Ciais P¹

7 ¹Laboratoire des Sciences du Climat et de l'Environnement, Commissariat à l'énergie
8 atomique / CEA-Orme des Merisiers / F-91191 Gif-sur-Yvette CEDEX / France

9 ²CIRAD, Persyst, UPR 80, s/c UMR Eco&Sols, 2 Place Viala - bât 12, 34060 Montpellier
10 cedex 01, France

11 ³Direction Technique et Commerciale Bois, Office National des Forêts / Boulevard de
12 Constance / 77300 Fontainebleau / France

13 **Corresponding author:** Bellassen V

14 Phone: +33 1 69 08 31 01

15 Fax:

16 E-mail: valentin.bellassen@lsce.ipsl.fr

17

18

19 **Abstract**

20 The construction of a new forest management module (FMM) within the ORCHIDEE
21 global vegetation model (GVM) allows a realistic simulation of biomass changes during
22 the life cycle of a forest, which makes many biomass datasets suitable as validation data
23 for the coupled ORCHIDEE-FM GVM. This study uses three datasets to validate
24 ORCHIDEE-FM at different temporal and spatial scales: permanent monitoring plots,
25 yield tables, and the French national inventory data. The last dataset has sufficient
26 geospatial coverage to allow a novel type of validation: inventory plots can be used to
27 produce continuous maps that can be compared to continuous simulations for regional
28 trends in standing volumes and volume increments. ORCHIDEE-FM performs better than
29 simple statistical models for stand-level variables, which include tree density, basal area,
30 standing volume, average circumference and height, when management intensity and
31 initial conditions are known: model efficiency is improved by an average of 0.11, and its
32 average bias does not exceed 25%. The performance of the model is less satisfying for
33 tree-level variables, including extreme circumferences, tree circumference distribution
34 and competition indices, or when management and initial conditions are unknown. At
35 the regional level, when climate forcing is accurate for precipitation, ORCHIDEE-FM is
36 able to reproduce most productivity patterns in France, such as the local lows of
37 needleleaves in the Parisian basin and of broadleaves in south-central France. The
38 simulation of water stress effects on biomass in the Mediterranean region, however,
39 remains problematic, as does the simulation of the wood increment for coniferous

40 trees. These pitfalls pertain to the general ORCHIDEE model rather than to the FMM.

41 Overall, with an average bias seldom exceeding 40%, the performance of ORCHIDEE-FM

42 is deemed reliable to use it as a new modelling tool in the study of the effects of

43 interactions between forest management and climate on biomass stocks of forests

44 across a range of scales from plot to country.

45 **Keywords:** model validation; global vegetation model (GVM); ORCHIDEE-FM; forest

46 management; carbon cycle;

47

48 **1 Introduction**

49 Global vegetation models (GVMs) simulate fluxes of carbon, energy and water in
50 ecosystems at the global scale, generally on the basis of processes observed at a plant
51 scale. Despite their correct ability to simulate hourly local (e.g., at flux tower sites) and
52 global seasonal to interannual (e.g., compared with atmospheric CO₂ observations)
53 variations in CO₂ fluxes, these models usually fall short of simulating biomass and soil
54 carbon pool dynamics within ecosystems (Desai et al., 2007; Viovy et al., in prep.; in
55 revision). This shortcoming has been attributed to forest age structure and
56 management, which are not simulated by most GVMs (Ciais et al., 2008). ORCHIDEE-FM,
57 a new GVM with an explicit representation of forest management practices typical of
58 European forests (Bellassen et al., this issue), addresses this challenge, but it has yet to
59 be validated against independent datasets.

60 Several of the many variables processed by GVMs can be measured and, thus, used for
61 validation: for example, leaf area index (Demarty et al., 2007), light absorption and light
62 use efficiency (Jung et al., 2007), carbon stocks (Masek and Collatz, 2006),
63 evapotranspiration (Thornton et al., 2002), and latent and sensible heat fluxes
64 (Abramowitz et al., 2008). However, validation exercises for GVMs most frequently
65 focus on carbon fluxes estimated with eddy-covariance techniques (Thornton et al.,
66 2002; Krinner et al., 2005; Turner et al., 2005; Schaefer et al., 2008).

67 Flux towers have two major strengths: the flux data that they deliver have a very fine
68 resolution in time, often half-hourly, and their reasonably large footprint of
69 approximately 100 ha (Nagy et al., 2006; Reichstein et al., 2007) averages the variability
70 due to individual trees. With regard to GVM validation, they also have two major
71 drawbacks. First, their costly structure and maintenance limits their numbers: large
72 networks such as FLUXNET manage to have good coverage of the different land-use
73 types and climates (Baldocchi et al., 2001), but they seldom provide clear insights on
74 inter-site variability within a given climate and land-use type. Therefore, it is difficult to
75 generalise measurements that could be heavily influenced by local conditions (e.g., soil
76 fertility or hydrological parameters) or management (e.g., recent thinning) (Lindner et
77 al., 2004). Second, because eddy-covariance technology is quite recent, the time-series
78 are seldom longer than one decade (Urbanski et al., 2007). This precludes the validation
79 of full stand rotations, which commonly last between 100 and 200 years, on temperate
80 forest ecosystems (Bottcher et al., 2008) unless flux towers are smartly distributed to
81 measure chronosequences (Amiro et al., 2006).

82 Thus, in their review of terrestrial carbon models, Hurtt et al. (1998) concluded that
83 GVMs need to be validated for a diverse range of spatial and temporal scales. Datasets
84 of forest stand structure variables (e.g., height, basal area, and volume increment) are
85 good candidates for this diversification because they are often available on wider spatial
86 and temporal scales than eddy-covariance data, but these variables are not simulated by
87 most GVMs. A new generation of GVMs that explicitly simulate forest management

88 begins to bridge this gap: Desai et al. (2007) validated the regional forest biomass
89 simulated by Ecosystem Demography with data derived from forest inventories in the
90 midwest United States, and Sato et al. (2007) compared the local age structure
91 simulated by SEIB-DGVM with intensive monitoring plots. However, to date, no GVM
92 has been evaluated simultaneously at the diverse spatial and temporal scales relevant
93 to managed forests.

94 Beyond the assessment of model error, a model validation exercise also provides the
95 opportunity for a better understanding of the model's strengths and pitfalls. In
96 particular, it should be designed to attribute a share of model error to each model
97 component. One way of attributing this model error is to quantify the improvement of
98 model fit when a given component is switched on. This approach was used by Zaehle et
99 al. (2006) for a model component simulating the processes involved in the age-related
100 decline of net primary productivity (NPP). Because it requires a validation variable that is
101 simulated both in the absence and presence of the component, this method is not
102 always applicable. Another way of attributing modelling error is to force a model by
103 replacing the outputs of one model component by site measurements. By assimilating a
104 satellite-derived leaf area index (LAI) in ORCHIDEE, Demarty et al. (2007) showed that
105 the phenology component of the model is responsible for 25% of the lack of fit to flux
106 tower data. Because the new forest management module (FMM) of ORCHIDEE
107 generates a whole new set of variables and processes, this second approach was found

108 to be better suited to discriminate between its error and the error coming from the
109 general core of ORCHIDEE.

110 In this study, we use forestry datasets to further evaluate the performance of the
111 ORCHIDEE-FM simultaneously at several spatial and temporal scales, which are all
112 relevant to the novelty introduced by the forestry management module, namely the
113 simulation of stand structure and its evolution with age. Two requirements are set for a
114 validation dataset:

- 115 • It should cover the diverse spatial and temporal scales necessary for exploring
116 regional variations and the full lifespan of a forest from harvest to harvest.
- 117 • It should provide the possibility to replace the input of ORCHIDEE to the FMM
118 with actual field values so that a share of modelling error can be attributed to
119 both the ORCHIDEE and the FMM components (see Figure 1).

120 No single dataset was found to match all of these requirements. Instead, we selected
121 three complementary datasets: permanent forest monitoring plots, yield tables, and
122 extensive forest inventory data (see Figure 2). Permanent plots provide long time series
123 and detailed within-plot measurements, but their spatial coverage is very limited. Yield
124 tables cover the entire European continent, but their precise area of relevance and
125 source data are often unknown. Inventory data is sufficiently abundant to create
126 spatially continuous maps of carbon stocks and stock changes (through surface tree
127 cores), but only one snapshot measurement is available for each plot. Here, these

128 datasets are successively compared to specific simulations to validate ORCHIDEE- and to
129 identify the most important sources of model error.

130 The notion of model validation is controversial (Oreskes et al., 1994). Confirmation that
131 models reproduce existing *in situ* measurements reasonably well is, nevertheless,
132 required of GVMs, the projections of which are used in the definition of climate change
133 mitigation and adaptation policy (IPCC, 2007). Therefore, we use the term of
134 “validation” with the cautionary requirements set by Rykiel (1996), clearly specifying the
135 model’s purpose, its context of operation and the criteria that it must meet for being
136 considered “acceptable for use”:

- 137 ✓ Model purpose: to simulate the age-related dynamics of carbon stocks and
138 fluxes that are ignored in the standard version of ORCHIDEE.
- 139 ✓ Context of operation: a tree to continental scale, limited to Europe.
- 140 ✓ Validation criteria: whereas plot-scale models, calibrated with site- and species-
141 specific parameters, can be expected to fit local data series, the aim of a GVM is
142 to simulate a regional average CO₂ flux, typically using 0.5° resolution. The
143 performance of ORCHIDEE-FM is, therefore, assessed through its ability to cut
144 across a cloud of data points corresponding to different sites in the same region.

145 All abbreviations used in this paper are indexed in Annex 1.

146 2 Material & Methods

147 2.1 ORCHIDEE and its forest management module (FMM)

148 2.1.1 Description of ORCHIDEE-FM

149 The ORCHIDEE global vegetation model (ORganising Carbon and Hydrology In Dynamic
 150 Ecosystems) was designed to operate from regional to global scales (Krinner et al.,
 151 2005). ORCHIDEE typically represents an average mature forest at steady-state
 152 equilibrium in a *big-leaf* manner. For a given climate, it simulates the carbon, water and
 153 energy budget at the pixel scale. For carbon, ORCHIDEE computes its fixation (gross
 154 primary productivity or GPP), allocates photosynthetates to the different biomass
 155 compartments where they are respired or stored, and recycles carbon through constant
 156 tree mortality and soil respiration. To simulate forest management, several processes
 157 have been added to the standard version of ORCHIDEE, among which is a forest
 158 management module (FMM) inspired by the stand-level model FAGACEES (Dhôte and
 159 Hervé, 2000). The key concept is to add to the “average tree” representation of
 160 ORCHIDEE an explicit distribution of individual trees, which is the basis for a process-
 161 based simulation of mortality (see Figure 1). The above-ground plot-scale wood
 162 increment simulated by ORCHIDEE is distributed among individual trees according to the
 163 rule of Deleuze et al. (2004):

$$164 \delta ba_i = \frac{\gamma}{2} \times \left(circ_i - m \times \sigma + \sqrt{(m \times \sigma + circ_i)^2 - 4 \times m \times \sigma \times circ_i} \right) \quad (1)$$

165 where δba_i is the annual increase in the basal area of tree i in square meters, and $circ_i$ is
 166 the circumference of tree i in meters. γ , σ and m are the slope, the threshold and the
 167 smoothing parameters, respectively (see Figure S1): trees whose circumference is lower
 168 than σ grow very little; thus, γ is the slope of the δba_i vs. the $circ_i$ relationship above σ .
 169 Then, tree mortality processes, due to natural competition, anthropogenic thinning or
 170 clear-cutting, rely on the self-thinning rule (Eq. 2) of Reineke (1933).

$$171 \quad dens_{max} = \frac{\alpha_{st}}{Dg^{\beta_{st}}} \quad (2)$$

172 where $dens_{max}$ is the stand maximum density in ind ha⁻¹ (individuals per hectare); α_{st} and
 173 β_{st} are parameters; and Dg is the quadratic mean diameter in m.

174 For more information on the structure of ORCHIDEE-FM, see Bellassen et al. (this issue).

175 **2.1.2 Pedo-climatic inputs and model “spinup”**

176 The climate data used in this study to drive ORCHIDEE is from the 0.25°-resolution
 177 REMO reanalysis covering the 1861-2007 period (Kalnay et al., 1996; Vetter et al., 2008).
 178 Maps of soil depth and texture were derived from FAO and IGBP products (Vetter et al.,
 179 2008). Following a standard method in GVM modelling, a model “spinup” is performed
 180 before all simulations to define the initial conditions from which subsequent simulations
 181 will be performed, in particular for soil carbon. For this “spinup”, ORCHIDEE and
 182 ORCHIDEE-FM are repeatedly run for the climate of the years 1861-1911 with a CO₂
 183 concentration of 280 ppm until all ecosystem carbon and water pools reach a cyclical

184 (clearcut-regrowth) steady-state equilibrium. The conditions of the stand after the last
185 clearcut are used as initial conditions for all ORCHIDEE-FM simulations.

186 **2.2 Validation data**

187 Three complementary datasets are used to validate the FMM and its integration in
188 ORCHIDEE: permanent plots, yield tables and national inventory. All three are necessary
189 to cover the three different scales of interest: tree scale (e.g., individual tree growth and
190 circumference distribution), stand scale (e.g., tree density and basal area), and
191 continental scale (e.g., inter-regional variations). The following paragraphs describe
192 each dataset and its specific use in our model validation assessment. Table 1
193 summarises the characteristics and aims of each simulation. Figure S 4, Figure S 5, and
194 Figure S 9 summarise measurements, simulations and validated variables for each of the
195 three datasets. The uncertainty associated to each dataset is discussed in part 2 of the
196 Supplementary Materials.

197 **2.2.1 Permanent plots**

198 *Description*

199 Fifty-eight permanent plots (PP) were set by the *Institut National de la Recherche*
200 *Agronomique* (INRA) for long-term monitoring of the evolution of forest stands (Dhôte
201 and Hervé, 2000). These plots contain either oaks or beeches. They all belong to even-
202 aged stands and were subject to different management intensities with a post-thinning

203 relative density index (*rdi*, see Eq. 3) ranging from 0.4 (heavy thinning) to 1 (no
204 anthropogenic thinning = unmanaged).

$$205 \quad rdi = \frac{dens}{dens_{max}} \quad (3)$$

206 where *rdi* is the relative density index, and *dens* and *dens_{max}* are the actual and maximal
207 tree densities, respectively, of the stand in ind.ha⁻¹.

208 *dens_{max}* is derived from Eq. 2. All trees in the plots are marked, and for each
209 measurement year, the status of trees is recorded (dead, alive, or thinned), as is their
210 circumference at breast height. Measured ages span 37-203 years, with an average
211 measurement frequency of 4.2 years.

212 A summary of permanent plot characteristics is provided in Annex 2.

213 *Estimation of non-measured variables*

214 The key variables of interest available at each plot for the validation of the FMM-
215 simulated counterparts are as follows:

- 216 • circumference distribution variables: minimum, average, and maximum
217 circumference as well as number of trees in a given circumference class
- 218 • stand variables: tree density and basal area.

219 Other variables, such as standing volume, standing biomass, tree height, wood
220 increment, and individual tree growth indicators (the σ and γ of Equation 1) can be
221 estimated. For detailed information on the estimation method, see part 1 of the
222 Supplementary Materials.

223 *PP_f and PP_c simulations: validation of tree-scale and stand-scale characteristics*

224 The *PP_f* (permanent plot-forced) simulation is aimed at validating tree-scale and stand-
225 scale characteristics between two measured states: the state of a stand at first
226 measurement and its state at last measurement. To validate the FMM separately from
227 the rest of ORCHIDEE, the annual increase in aboveground woody biomass (*wood_{inc}*) is
228 forced by the *in situ* estimate instead of the value simulated by the core of ORCHIDEE.

229 The initial conditions of *PP_f* are the conditions of each permanent plot at its first
230 measurement regarding tree circumferences and, therefore, aboveground biomass. The
231 other biomass compartments (e.g., leaves, roots, and soil) are not used as inputs in the
232 FMM and, therefore, do not need to be accounted for when the FMM is forced.

233 The aim of the *PP_c* (permanent plot-coupled) simulation is to assess the additional error
234 brought to the FMM outputs by an initial error in the simulation of stand-scale wood
235 increment by ORCHIDEE. *PP_c* is therefore similar to *PP_f*, except that the FMM is no
236 longer forced by data-derived *wood_{inc}*. Instead, the coupled ORCHIDEE-FM model is run
237 over the measurement period of each plot using the corresponding climate forcing to
238 provide a simulated *wood_{inc}*. Whereas the differences between *PP_f* and the data reveal
239 the error of the FMM in simulating management and growth distribution, those
240 between *PP_c* and *PP_f* reflect the error due to the simulation of *wood_{inc}* by ORCHIDEE.

241 Comparing the performance of *PP_f* vs. *data* to that of *PP_c* vs. *PP_f* allows us to attribute a
242 share of the total error (*PP_c* vs. *data*) to each of the model's components. Comparing *PP_c*
243 directly to the data would be confusing because the error of each component might

244 cancel each other out and, consequently, be wrongly interpreted as a high modelling
245 efficiency.

246 *PP_{fi} simulation: validation of initial distribution*

247 The *PP_f* (permanent plots initial conditions) simulation complements the *PP_f* simulation
248 by assessing the model's ability to reproduce the state of each plot at its first
249 measurement, starting from the default model initial conditions of 10,000 trees per
250 hectare, with circumferences following a decreasing exponential distribution (Bellassen
251 et al., this issue). The FMM is, therefore, run on each permanent plot from its date of
252 regeneration until the first measurement year. For the *PP_f* simulation, the FMM is
253 decoupled from the rest of ORCHIDEE: the annual increase in aboveground woody
254 biomass between year one and the first measurement is forced by the average annual
255 wood increment estimated from field data over the measured period.

256 **2.2.2 Yield tables**

257 *Description*

258 More than a thousand forest yield tables have been compiled by the Joint Research
259 Centre (JRC, 2009). They cover 26 European countries and 23 genuses. Forest yield
260 tables give the evolution of typical stand variables, including tree density, basal area,
261 dominant or average height, average circumference, standing volume and thinned
262 volume, with age. All of these variables will be tested against FMM simulations for
263 validation. Yield tables are usually established based on either permanent plots

264 monitored over an entire rotation, or temporary plots of different ages monitored once.
 265 Their aim is to reproduce the average growth pattern of a tree species in a given region,
 266 which sometimes declines in *yield classes* representing different levels of treatment or
 267 local fertility. Because the FMM simulates the growth of an average coniferous or
 268 broadleaf species managed as a high stand, coppices and fast-growing poplars and
 269 eucalypts were discarded from the database. When needed, cormometric volume
 270 (merchantable volume) was converted into dendrometric volume (whole tree) using a
 271 branch to total volume ratio of 0.25 for needleleaf species and 0.38 for broadleaf
 272 species (Loustau, 2004).

273 *Testing the effect of climate and management in the dataset*

274 Yield tables complement permanent plots by providing a presumably much more
 275 diverse range of climates, species and management conditions. However, neither
 276 management style nor climate are represented by explicit indicators as is the case with
 277 permanent plots for which accurate location, plot age and the targeted relative density
 278 index play that role. A first step in testing the FMM against this assumed variety of
 279 climates and management conditions is therefore to test whether climate and
 280 management effects can indeed be detected in the dataset. To test the climate effect,
 281 an analysis of variance was performed using the mixed linear model of Eq. 4.

$$282 \text{vol}_{tot}(i, j, k) = \alpha + \beta_i + \gamma_j + \varepsilon(i, j, k) \quad (4)$$

283 where α is the intercept; β_i and γ_j are the coefficients associated with plant functional
 284 type (PFT) i and country j , respectively, and $\text{vol}_{tot}(i, j, k)$, and $\varepsilon(i, j, k)$ are the total volume

285 produced at year 80 and the error term associated with yield table k of PFT i and
 286 country j, respectively. The error terms $\varepsilon(i,j,k)$ are assumed to be dependent upon the
 287 yield table k, justifying the use of a linear mixed model with PFT and country as fixed
 288 effects.

289 Because the total biomass (standing biomass + thinned biomass) produced by a plot is
 290 largely independent of the management style (Lanier, 1994), this variable was not suited
 291 to test the diversity of management styles in the data. For this purpose, a second
 292 analysis of variance based on tree density was performed using the linear mixed model
 293 of Eq. 5.

$$294 \quad dens(i, j, k) = \alpha + \beta_i + \gamma_j + \delta \times vol_{tot}(i, j, k) + \varepsilon(i, j, k) \quad (5)$$

295 where α is the intercept; β_i , γ_j and δ are the coefficients associated with plant functional
 296 type (PFT) i, country j, and total volume produced at year 80, respectively; $dens(i,j,k)$,
 297 $vol_{tot}(i,j,k)$ and $\varepsilon(i,j,k)$ are the density, the total volume produced at year 80 and the
 298 error term associated with yield table k of PFT i and country j, respectively. The error
 299 terms $\varepsilon(i,j,k)$ are assumed to be dependent upon the yield table k, justifying the use of a
 300 linear mixed model.

301 Density is highly dependent on management for a given productivity level, which is
 302 embedded in the random factor vol_{tot} , and management is, therefore, likely to explain
 303 most of the variance attributed to country and PFT when productivity is already
 304 captured by another variable (here vol_{tot}). In this model, β and γ can thus be interpreted
 305 as indicators of the country- and PFT-specific variation in management style.

306 *YT_f simulation: validation of stand-scale characteristics across Europe*

307 The *YT_f* (yield tables-forced) simulation is aimed at validating stand-scale characteristics
308 across Europe. As in the *PP_f* simulation, the annual increase in aboveground biomass is
309 forced by the mean annual increment given in the yield table to validate the FMM
310 separately from the rest of the ORCHIDEE model. However, because the yield tables do
311 not provide initial conditions with enough detail, the initial conditions of the *YT_f*
312 simulation are set to the default model initial conditions, as in the *PP_{fi}* simulation. To
313 bridge the data gap between age 0 and the first age of the yield table, which varies
314 between 5 and 20 years, the mean annual increment during this period is set to add up
315 to the first data on total volume.

316 **2.2.3 French national inventory**

317 *Description*

318 The French National Forest Inventory (NFI) conducts yearly field measurement
319 campaigns covering the entire French metropolitan territory. Each intersection of a
320 systematic grid of 10 x 10 km² is photo-interpreted to determine land cover and land-
321 use. Of these intersections, every other forested point, totalling about 8 000 points per
322 year, is visited and inventoried following the NFI protocol (IFN, 2006): circumference at
323 breast height, width of the last five rings, height and species are recorded for a
324 representative sample of trees. NFI allometric rules are used to estimate tree volume
325 and annual volume increment, and all of these data provide the basis for an estimate of

326 plot-scale tree density, basal area, dominant height, standing volume and the annual
327 volume increment. For even-aged stands, a few trees are cored to the stem centre to
328 estimate stand age. For this study, we pooled together the results of three campaigns
329 (2005, 2006 and 2007). Because the FMM only represents even-aged high stands, all
330 other management types were excluded from the analysis. Our sample size was,
331 therefore, reduced to 11,222 sites. The raw data are available on the IFN website:
332 www.ifn.fr.

333 *Interpolation*

334 Both permanent plots and yield tables are unsuitable to test the ability of ORCHIDEE-FM
335 to simulate regional trends in carbon stocks and fluxes. Thus, a spatially continuous
336 dataset is needed. With its high spatial density, the NFI dataset presents the opportunity
337 to build continuous maps: for the category of broadleaf plots of the 80-100 years age
338 class alone, half the French territory has at least 10 plots within a distance of 0.5° (55
339 km), and only 24% of the territory has less than 5 plots. However, this dataset is
340 heterogeneous: the order of magnitude of the standard deviation of the volume
341 increment within a radius of 0.5° is 30%. Therefore, a smoothing is necessary to
342 eliminate the local variations due to topography, soil fertility and species composition
343 and to retain only the regional climate-related variations in carbon stocks and fluxes.
344 Several interpolation techniques were tested to obtain these smoothed data-derived
345 maps, resulting in the joint use of the following two methods:

- 346 • *Large footprint interpolation technique*: the data were interpolated with a
347 minimum footprint radius of 0.5° and no distance weighting. Where necessary,
348 the footprint was extended to include a minimum of 10 plots. The result is a
349 0.05° resolution map for which each final pixel represents the average of all plots
350 within a 0.5° radius of the centre of the pixel.
- 351 • *Data density mask*: density masks were created to distinguish pixels with more
352 than 10 plots within a 0.5° radius. Applying these masks restricts model-data
353 comparisons to the areas where the uncertainty in the data is lowest.

354 *NFI_{std} and NFI_{fmm} regional simulations*

355 Two types of simulations were conducted to assess the model's ability to reproduce the
356 trends observed in the NFI data.

- 357 • The *NFI_{std}* simulation aims at representing an average forest at steady-state
358 equilibrium, typical of GVMs. Thus, the standard version of ORCHIDEE was run
359 between 1956 and 2006, which is the average measurement year for the dataset
360 (2005-2007).
- 361 • The three *NFI_{fmm}* simulations aim at validating the coupled version of the
362 ORCHIDEE-FM. The model was run for 50, 90, and 130 years with all runs ending
363 in 2006. The resulting *NFI_{fmm50}*, *NFI_{fmm90}*, and *NFI_{fmm130}* results can, thus, be
364 compared to NFI plots of three selected age-classes: 40-60 years, 80-100 years

365 and 120-140 years. In both cases, the CO₂ concentration follows its historical
366 increase from 290 ppm in 1876 to 378 ppm in 2006.

367 The wood increment estimated in the NFI data comes from surface cores of live trees. It
368 is a gross commercial wood increment, and it does not account for woody losses from
369 artificial thinning or natural mortality. From the simulation of tree-level growth and
370 mortality, a similar variable can be extracted from the ORCHIDEE-FM simulations,
371 allowing its validation. The commercial wood increment is converted to the total wood
372 increment using the relevant PFT-specific branch expansion factor (BEF) of IPCC (2003).
373 “Difference maps” present the relative difference between each pixel of data-derived
374 maps and its closest simulation point. These maps are limited to pixels complying with
375 the data density masks, which are pixels with at least 10 inventory plots within a 0.5°
376 radius of the centre of the pixel.

377 *NFI_{opt} and NFI_{st} simulations for error attribution*

378 Unlike permanent plots, it is not possible to estimate the history of productivity in each
379 NFI plot. The only data point available is the average tree-ring width over the previous
380 five years that is obtained from a surface core. Therefore, attributing error to the
381 management or productivity simulation is not straightforward when one is looking at
382 cumulative variables such as standing biomass. To do so, two additional types of
383 simulations are performed:

- 384 • For the *NFI_{opt}* simulations, we replaced the default values of the photosynthesis
385 efficiency parameters ($v_{c_{max}}$, the maximum capacity of the Rubisco enzyme, and

386 $v_{j_{\max}}$, the maximum regeneration speed of the Rubisco enzyme) with the values
 387 of Santaren (2006), who optimised their ORCHIDEE model based on eddy-
 388 covariance measurements from six European sites. Broadleaves were
 389 unaffected, but the photosynthesis efficiency of needleleaves was increased by
 390 20%. NFI_{opt} simulations are a sensible variant of NFI_{fmm} simulations for
 391 productivity.

- 392 • For the NFI_{st} simulations, artificial thinning is disabled, and only self-thinning
 393 occurs, thus representing the minimal level of management. When a lack of fit
 394 between the ORCHIDEE-FM and data for standing biomass comes from overly
 395 intensively simulated management, NFI_{st} provides a comparison with the most
 396 extensive type of management.

397 **2.3 Criteria of model performance**

398 Two common criteria are used to evaluate model performance: EF , model efficiency,
 399 and AB , model average relative bias (Soares et al., 1995; Smith et al., 1997). Their
 400 definition is given by Eq. 6 and 7.

$$401 \quad EF = 1 - \frac{\sum_i (mes_i - sim_i)^2}{\sum_i (mes_i - \overline{mes})^2} \quad (6)$$

$$402 \quad AB = \frac{1}{n} \sum_{i=1}^n \frac{(sim_i - mes_i)}{mes_i} \quad (7)$$

403 where mes_i and sim_i are the measured data point i and its simulated counterpart,
 404 respectively; \overline{mes} is the data average; and n is the number of data points.

405 EF reflects the ability of the model to reproduce the data: the closer it gets to 1, the
 406 better the fit. AB indicates whether the model has a systematic bias. Whereas an
 407 efficient model necessarily has a small systematic bias, the reverse is not always true.
 408 However, when a large-scale model such as ORCHIDEE is compared to plot-scale
 409 measurements, avoiding systematic bias may be more important than scoring high
 410 efficiency: large-scale models are not expected to reproduce each stand specifically but
 411 rather to simulate an “average stand” within the gridcell of interest.

412 To improve the interpretation of these criteria, we undertook three complementary
 413 analyses:

- 414 • “Shadow models”: for each simulation, we built a “shadow model” for the
 415 ORCHIDEE-FM. These “shadow models” are simple statistical models using the
 416 same input variables as ORCHIDEE-FM. For the stand-scale variables of the PP_f
 417 simulation, for example, the main input variables of ORCHIDEE-FM are total
 418 volume, initial conditions (initial median circumference), and management
 419 intensity (post-thinning relative density index). The shadow model thus follows
 420 Eq. 8.

$$421 \quad mes(i) = a \times vol_{tot}(i) + b \times med_{circ}(i) + c \times rdi_{target}(i) + \varepsilon(i) \quad (8)$$

422 where mes is the measured variable of interest (e.g., tree density and standing
 423 volume); vol_{tot} is the total volume of the stand at the last measurement; med_{circ}
 424 is the median circumference of the stand at the first measurement; rdi_{target} is the
 425 post-thinning relative density index; a , b , c , and d are regression coefficients; i is
 426 the permanent plot number; and $\varepsilon(i)$ is the error term associated with $mes(i)$.

427 “Shadow models” are calibrated on one half of the dataset, and their efficiency
 428 (EF_{stat}) is assessed on the other half. The details of each model and its calibration
 429 are presented in the Supplementary Materials.

430 • Systematic vs. unsystematic error: to assess the importance of the average bias,
 431 we computed the systematic ($RMSEs$) and unsystematic ($RMSEu$) errors of
 432 Willmott (1982), defined by Eq. 9 and 10, respectively:

$$433 \quad RMSEs = \frac{1}{n} \sqrt{\sum_{i=1}^n (pred_i - mes_i)^2} \quad (9)$$

$$434 \quad RMSEu = \frac{1}{n} \sqrt{\sum_{i=1}^n (pred_i - sim_i)^2} \quad (10)$$

435 where $RMSEs$ and $RMSEu$ are the systematic and unsystematic root mean square
 436 error, respectively; n is the number of the measurement; sim is the simulated
 437 variable; mes is the measured variable; i is the measurement number; and $pred$
 438 is the value predicted by the linear regression $sim = f(mes)$: $pred_i = a + b \times mes_i$,
 439 where a and b are the regression coefficients.

440 $RMSEs$ represents the error due to a systematic bias in the model, and $RMSEu$
 441 represents the “random” error. The $RMSEs/RMSEu$ ratio places the average

442 relative bias in perspective: even a large AB is not very meaningful if the
 443 $RMSEs/RMSEu$ ratio is lower than one.

444 • Error share of a given model component: an index (ES_{fmm}) of the share of the
 445 total error of ORCHIDEE-FM that can be attributed to the FMM component was
 446 computed based on the permanent plots data as well as the PP_f and PP_c
 447 simulations (see Eq. 11).

$$448 \quad ES_{fmm} = \frac{1 - EF_{PPf}}{(1 - EF_{PPf}) + (1 - EF_{PPc})} \quad (11)$$

449 where ES_{fmm} is the error share of the FMM model component (0 when all of the
 450 error comes from ORCHIDEE and 1 when it comes entirely from the FMM), and
 451 EF_{PPf} and EF_{PPc} are the efficiency of PP_f to reproduce the data and the efficiency
 452 of PP_c to reproduce the PP_f simulation, respectively.

453 **3 Results**

454 **3.1 Stand scale: stand characteristics**

455 **3.1.1 Permanent plots**

456 *PP_f and PP_{fi} simulations: good performance of the FMM under controlled conditions*

457 Average stand characteristics such as tree density, basal area, average circumference
 458 and standing volume are efficiently simulated under the control conditions of PP_f (Figure
 459 3 and Figure 4). All of these characters have modelling efficiencies higher than 0.5 and

460 average biases below 20%. This average bias is negligible because the systematic error is
461 smaller than the unsystematic error: all $RMSEs$ to $RMSEu$ ratios are lower than 0.6
462 (Table 2). The model is not as accurate for extreme circumferences: both have lower
463 efficiencies, and the minimum circumference is consistently underestimated with an
464 average bias of -25% and a systematic error component overtaking the unsystematic
465 component. These deficiencies essentially occur for plots with large trees (Figure 3).
466 With the approximations necessary for the PP_{fi} simulation (default model initial
467 distribution and average growth rate), the fit of all variables deteriorate. Except for
468 standing volume and average circumference, all model efficiencies become negative.
469 From the results of the PP_{fi} simulation, we conclude that the model could not correctly
470 reach the initial state of the PP_f simulation. Average biases are also higher than for the
471 PP_f simulation, although none exceeds 45%. However, because all $RMSEs$ to $RMSEu$
472 ratios remain below 0.7, the default initial conditions of ORCHIDEE-FM can be
473 considered to induce no strong systematic bias to the simulations. For both simulations,
474 the FMM is more efficient than its simple statistical “shadow models”. For stand-scale
475 variables, its efficiency is on average of 0.11 higher for PP_f and 0.6 higher for PP_{fi} .
476 *PP_f and PP_c simulations: a minor share of modelling error for the FMM component*
477 The (inaccurate) simulation of wood increment by ORCHIDEE is a more important source
478 of error than the processes simulated by the FMM. For most variables, the forced FMM
479 (PP_f) is more efficient at reproducing the data than ORCHIDEE-FM (PP_c) is at reproducing
480 the forced FMM (Figure 4). For basal area, which is the variable most commonly

481 estimated by forest inventories, the efficiency of the forced FMM to reproduce the data
482 is three times higher than that of ORCHIDEE-FM to reproduce the forced FMM, giving an
483 ES_{fmm} value of only 35%. Because the efficiency of the coupled PP_c remains quite high for
484 standing volume, the error for this variable is, therefore, split evenly between ORCHIDEE
485 and the FMM ($ES_{fmm} = 48\%$).

486 **3.1.2 Yield tables**

487 *Statistically significant effect of climate and management practices in the dataset*

488 The statistical model of Equation 4 explains 64% of the total variance, and both country
489 and PFT predictors have a significant effect (p -value < 0.001) on the total volume
490 produced (the detailed statistics are provided in the Supplementary Materials).
491 Therefore, the effect of climate is present, though blurred, in the yield table dataset.
492 This result can be ascertained visually from Figure 5: the estimated coefficients for
493 country (γ_j), representing the relative effect of each country corrected for PFT effects,
494 present a climatic pattern with lower values in arid Spain and the cold Russo-
495 Scandinavian countries. This pattern is clearly blurred over western and central Europe,
496 where the differences between countries are difficult to explain based on climate alone.
497 The statistical model of Equation 5 explains 47% of the total variance, and all
498 explanatory variables (country, PFT, and total volume produced) have a significant effect
499 (p -value < 0.01) on stand density. The effect of the total volume produced is, as
500 expected, more important than that of PFT and country (F-value is about 50 times

501 higher for total volume). Because management style is expected to vary between PFTs
502 and countries, this result points to a detectable effect of management style on tree
503 density, although other explanations for the effect of PFT and country cannot be
504 discarded (e.g., ecophysiological differences between PFTs and differences in
505 methodology for establishing yield tables between countries). Similar results are
506 obtained if density is replaced by basal area or standing volume in Equation 5, showing
507 that management styles also affect these two variables.

508 *YT_f simulation: validation across a variety of management and climate conditions*

509 Except for tree density, average biases do not exceed 55% for the *YT_f* simulation, and
510 most modelling efficiencies are higher than 0.3, with the exception of average height
511 and average circumference (Figure 6 and Figure 7). The FMM performs particularly well
512 for standing volume with an EF value of 0.83 and an average bias of only -2%. This value
513 is slightly better than the “shadow model” (EF_{stat} = 0.82, AB_{stat} = 16%, see Table 2).

514 Because standing volume varies little for a given level of total volume produced, the
515 linear regression is indeed more sensitive to extreme values, which may differ between
516 the calibration and test subsamples and produce a higher average bias in the shadow
517 model.

518 For most variables, however, the performance of the FMM is lower for *YT_f* than under
519 the highly controlled conditions of *PP_f*. Efficiencies are lower and average biases are
520 higher, as is the systematic to unsystematic error ratio; however, it remains below 1 for
521 all variables except average height.

522 The FMM does not efficiently simulate tree density (EF = -8). In particular, it
 523 overestimates high densities. However, the average bias of +160% is not uniform: Figure
 524 6 shows that the fit is best for low densities (around 600 trees.ha⁻¹), meaning that the
 525 average bias comes from the high number of data points from the high densities where
 526 the bias is particularly high, rather than a systematic bias spanning the entire density
 527 range. The average bias of +96% in the shadow model shows that reproducing the tree
 528 density trends from the yield tables is not easy to accomplish. This difficulty could
 529 originate from a specific treatment effect or measurement errors for the higher tree
 530 densities.

531 **3.1.3 French national inventory**

532 *Interpolated NFI plots and NFI_{fmm} simulations: regional trends*

533 The interpolation technique unearths regional differences in volume increments (Figure
 534 8a and Figure 8c), most of which are bolstered by a large number of plot measurements.
 535 For broadleaves, the range of the volume increment is from 2 to 18 m³.ha⁻¹yr⁻¹, half that
 536 of the needleleaves, which can grow as fast as 30 m³.ha⁻¹yr⁻¹ in northeastern France. In
 537 particular, regional lows of -48% and -59% in the Mediterranean region (2)¹ can be
 538 observed, extending somewhat inland toward south-central Toulouse to the west for

¹ To help readers unfamiliar with French geography, numbers between brackets refer to the regional markers of Figure 8d. The exact boundaries of these “regions” are given in **Erreur ! Source du renvoi introuvable.** of the Supplementary Materials.

539 broadleaves (3, -21%), and from the mid-Atlantic coast (7, -12% and -26%) to the
540 Parisian basin for needleleaves (1, -10%). Robust regional highs occur in northeastern
541 France (4, +36% for both) for both functional plant types, in Brittany (5, +5%) for
542 needleleaves and at the southwestern tip (6, +15%) for broadleaves.
543 The sign of these regional trends in volume increment is generally correctly simulated
544 (see Table 4). However, the amplitude of these variations is often underestimated; in
545 particular, the regional high in the north-eastern region (4) and the regional low for the
546 Mediterranean (2) are both underestimated in the simulations (Figure 8b and Figure
547 8d).

548 *Model fit for different age classes*

549 Leaving the Mediterranean region aside, the simulated broadleaf increments are
550 generally within the 20% uncertainty associated with the data-derived map (Figure 9).
551 The increment is, nevertheless, slightly underestimated around Paris and in the
552 southwest, by 20% and 50%, respectively. On the contrary, needleleaf increments are
553 systematically underestimated by at least 20% and often by more than 50% with the
554 exception of the southwest (6). For both plant functional types, the volume increment is
555 largely overestimated for the Mediterranean region.

556 *Improvement in the simulation of biomass*

557 For 50-year-old broadleaves, the standard version of ORCHIDEE (NFI_{std50}) overestimates
558 standing volume, which is directly related to aboveground biomass stocks through wood
559 density, by an average of 60% (Figure 10a and Figure 10c). ORCHIDEE-FM (NFI_{fmm50}) is

560 much closer to the data (Figure 10b), with an average underestimate of -16%. This
561 pattern is also true for needleleaves at the southwestern tip of France (Figure 11a). For
562 the rest of the country except for the Mediterranean region, the standing volume is
563 systematically underestimated. When productivity is optimised in NFI_{opt50} , model fit
564 improves in some regions at the expense of others (Figure 11b). The same happens
565 when management is made more extensive with no artificial thinning (Figure 11c). Only
566 when productivity optimisation is combined with reduced management intensity in
567 NFI_{opt_st50} can the high volumes measured in central and northeastern France be
568 reproduced in the model (Figure 11d). This result reflects the lesser intensiveness of
569 management in these mountainous areas. A similar pattern in data-derived rdi confirms
570 this interpretation (Figure S 8).

571 **3.2 Tree scale: individual tree growth and circumference distribution**

572 **3.2.1 Individual tree growth**

573 The FMM model imperfectly reproduces individual tree growth variables as measured
574 on the permanent plots (Figure 12). Both σ and γ have low model efficiencies of 0.1 and
575 -0.3, respectively, and γ is even significantly overestimated. However, both simulated
576 variables vary within the correct range of values, and their average biases of around
577 15% are not alarmingly high given the low efficiencies. The relevant “shadow models”
578 are also very inefficient, suggesting that the current input variables are not sufficient to
579 correctly predict these variables. Thus, the simulation of σ and γ will be difficult to

580 improve without a more detailed representation of inter-tree competition processes.
581 This representation would require an additional level of complexity and site-specificity
582 in the FMM, which is not compatible with the aimed generality of ORCHIDEE-FM.

583 **3.2.2 Circumference distribution**

584 When permanent plots are sorted by increasing the simulated proportion of trees in the
585 greater than 1.4-m circumference category (Figure 13), a similar trend towards larger
586 circumference classes appears in the observed circumference distributions. This trend
587 shows that the model can capture the inter-plot differences in circumference
588 distribution. The trend in the data however, is blurred by several plots with a high
589 proportion of narrower trees than simulated. Some of these are merely attenuated in
590 the simulations (e.g., plots n°14-21-26), suggesting that circumference distribution is
591 essentially driven by the volume increment, with the FMM slightly overestimating tree
592 growth for lower values of the volume increment. In other cases, the high proportion of
593 narrower trees is not simulated at all (e.g., plots N°6-46-47-55). In these cases,
594 circumference distribution is probably driven by other factors that are not modelled in
595 the FMM (e.g., a high level of competition for light due to local topography or a “from
596 above” thinning strategy).

597 **4 Discussion**

598 ***4.1 Effect of climate and management on carbon stocks and fluxes***

599 **4.1.1 Regional assessment of carbon fluxes**

600 The introduction of management and tree-level mortality into a GVM allows us to
601 validate carbon stocks and stock changes on continuous maps derived from the spatially
602 abundant inventory data. To our knowledge, this type of validation is a first for a GVM.
603 It complements the validation of short-term CO₂ fluxes at flux towers. Although the
604 inventory data only has a five-year resolution in time, it uncovers regional variations in
605 carbon fluxes that are very difficult to capture with flux towers. In particular, the low
606 productivity of the Parisian basin and the high productivity of northeastern France that
607 were detected in the data are correlated with pockets of low and high precipitation,
608 respectively, in particular for the five years before 2006. The mixed performance of
609 ORCHIDEE-FM in simulating these pockets is partly due to the mediocre accuracy of the
610 climate forcing data: while the REMO reanalysis clearly shows a regional low in
611 precipitation over the Parisian basin, it does not reproduce the pockets of higher
612 precipitation in the northeast (Meteo-France, 2009). This shortcoming combined with a
613 similar one in soil data (depth and texture) explains that simulations have a lower
614 amplitude of spatial variation than averaged measurements. Another reason for this
615 lower amplitude is the structure of the model itself. ORCHIDEE probably underestimates
616 water stress in the Mediterranean context (Morales et al., 2005; Gervois et al., 2008). In

617 northeastern France, an area with high nitrogen deposition, the model's inability to
618 simulate the high observed values in the volume increment partly comes from the
619 absence of an explicit simulation of the nitrogen cycle.

620 Some larger-scale patterns, however, can be found in both the inventory and eddy-
621 covariance data. Using eddy-covariance data, Luyssaert et al. (2007) found that
622 precipitation drives NPP when average yearly temperature is higher than 10°C. Because
623 only a few mountainous grid cells (less than 10%) have an average temperature lower
624 than 10°C in France, this rule is consistent with our previous observation that
625 precipitation drives most regional trends in the country, both in data-derived maps and
626 simulations.

627 These comparisons between eddy-covariance-based and inventory-based validations
628 must, nevertheless, be made cautiously. Flux towers measure whole-stand NEE (and
629 GPP through flux-separation algorithms), while forest inventories estimate the share of
630 NPP allocated to above-ground woody growth ($wood_{inc}$) over a time period of several
631 years. Both variables are strongly correlated, but a model with a faulty allocation
632 scheme could perform well for total GPP and badly for $wood_{inc}$. However, the joint use
633 of both methods presents new opportunities for the separate validation of production
634 and allocation processes.

635 **4.1.2 Optimisation of biophysical parameters**

636 Another key result from this spatially continuous validation is the rescaling from an
637 optimisation of photosynthesis efficiency parameters for needleleaves. Using the
638 optimised parameter values of Santaren (2006) improves model fit, but this does not
639 prove sufficient for all regions: rescaling allocation, plant respiration or management
640 intensity parameters also seem necessary. The model better reproduces the estimated
641 standing volume in southwestern France, which is not surprising: the parameters of
642 ORCHIDEE are based on published experimental studies, which are much more
643 abundant for southwestern *Pinus pinaster* than for northeastern *Abies alba* and *Picea*
644 *abies*. Our results question the generality of this parameterisation. Although this
645 optimisation of maximum photosynthesis rates is very coarse, the results are
646 qualitatively similar to the much finer GVM-oriented optimisation of $v_{C_{max}}$ using leaf
647 nitrogen content that was carried out by Kattge et al. (2009). This optimisation was
648 indeed an large upward correction from the original values of Beerling and Quick (1995)
649 for temperate needleleaves (see Table 5).

650 **4.1.3 Management intensity maps**

651 Management variability has also been shown to be an important driver of stand
652 characteristics and carbon stocks, both at regional (forest inventory) and continental
653 (yield tables) scales. In particular, management intensity has been shown to play a
654 comparable role to photosynthesis efficiency in explaining regional patterns of standing
655 volume. This result suggests that the performance of GVMs could be significantly

656 improved if management and photosynthesis efficiency were allowed to vary regionally
657 instead of having unique PFT-specific parameterisation. Such a regional
658 parameterisation would be feasible in Europe, where management intensity and species
659 distribution can potentially be mapped (Nabuurs et al., 2008).

660 ***4.2 Simulating endogenous heterogeneity in a GVM***

661 In the field of ecological modelling, a common distinction exists between exogenous
662 heterogeneity, which arises from abiotic components such as climate or soil type, and
663 endogenous heterogeneity, such as the heterogeneity in individual tree circumferences,
664 which exists even in physically homogenous environments (Moorcroft et al., 2001). The
665 validation of ORCHIDEE-FM highlight the use of simulating such fine-scale processes in
666 large-scale GVMs. Although the endogenous heterogeneity now represented by the new
667 model structure with extreme circumferences, competition indexes, and circumference
668 distribution, is inefficiently simulated by ORCHIDEE-FM, the process-based model
669 outperforms simple statistical models for stand-level variables such as basal area and
670 standing volume. A similar pattern is found for the stand-level FORSKA model (Lindner
671 et al., 1997). This similarity suggests that a correct average representation of
672 endogenous heterogeneity is better than none at all, even if it poorly matches the data
673 on a plot per plot basis. Moreover, the process-based simulation of endogenous
674 heterogeneity presents the possibility to assess the impact of concrete management
675 decisions, such as short rotations, high thinning intensity, and high thinning frequency,
676 on carbon stocks and fluxes at large scales.

677 **4.3 Model strengths and limitations**

678 **4.3.1 Model robustness for basal area and standing volume**

679 The validation results for the yield tables show that despite a significant impact of
680 management styles in the data, the simulations are quite efficient and not strongly
681 biased, in particular, for standing volume and basal area. Similar conclusions can be
682 drawn from the *NFI_{fmm}* simulations for broadleaf standing volume. The performance of
683 ORCHIDEE-FM for basal area and standing volume probably has two explanations: first,
684 the model is robust to changes in management parameters for these variables, as
685 shown by the sensitivity analysis of Bellassen et al. (Bellassen et al., this issue), and
686 second, basal area and standing volume are less heavily influenced by local conditions
687 than other variables such as average diameter or tree density and, therefore, respond
688 more directly to the large-scale climatic variations driving GVMs like ORCHIDEE (Wang et
689 al., 2006). Overall, this robustness justifies the rationale for management simulation in
690 GVMs, namely that simulating an “average” management is more realistic than not
691 simulating management.

692 **4.3.2 Tree density and self-thinning curves**

693 The performance of ORCHIDEE-FM to simulate tree density and average diameter is
694 much worse when the initial conditions and management style are unknown. The
695 proportion of systematic error for these two variables is twice as high as for basal area

696 or standing volume in the YT_f simulation, whereas they are comparable for all four
697 variables in the PP_f simulation. There are two likely reasons for this systematic error:

- 698 • The self-thinning curves of ORCHIDEE-FM are not generic enough. Although
699 Reineke (1933) originally thought that site or species productivity made no
700 difference to his equations and would only accelerate the self-thinning process,
701 this has recently been questioned (Yang and Titus, 2002; Vacchiano et al., 2008).
702 Needleleaves tolerate higher densities than broadleaves, thus suggesting an
703 effect of at least plant functional type, if not species, on self-thinning curves
704 (Figure 14). For needleleaves, the default self-thinning curve of ORCHIDEE-FM
705 seems to be generic enough because it encompasses yield table data for the
706 entire productivity range (total volume produced at year 80). However, this is
707 not the case for broadleaves, for which many productive yield tables lie above
708 the curve: some broadleaf species may, thus, be more tolerant to crowding than
709 the oaks and beeches on which the self-thinning curve was established (Dhôte,
710 1999).
- 711 • The management style varies with density. Indeed, Figure 14 suggests that
712 management may be more intense when the stand is dense. For both plant
713 functional types, the data-derived thinning curve cuts across the simulated
714 values as the stand grows sparser. Different management styles and intensities
715 between European countries could explain the important variability of the data.

716 These results highlight the important contributions that empirical studies of self-
717 thinning and thinning curves could make to the performance of ORCHIDEE-FM, which
718 has already been shown to be very sensitive to these parameters (Bellassen et al., this
719 issue). Another approach would be to construct a data assimilation framework for
720 ORCHIDEE-FM to optimise the thinning and harvest parameters on existing wood
721 production datasets.

722 **4.3.3 Bridging the gap with raw inventory data: basal area increment**

723 One of the original ideas in ORCHIDEE-FM is its ability to put a process-based GVM on
724 par with forest inventory data. In terms of proxy variables for productivity, ORCHIDEE-
725 FM performs better for the volume increment than for the basal area increment. This is
726 mainly due to the lack of performance of ORCHIDEE-FM at the tree scale: the basal area
727 increment is very dependent on tree circumference distribution because many small
728 trees will show a higher basal area increment than a few large trees for the amount of
729 volume increment. Therefore in this study, we used the estimated volume increment
730 from the French inventory instead of the measured basal area increment. If the same
731 validation exercise was undertaken at the European scale, then the basal area
732 increment might be the only option because the methods for estimating volume vary
733 strongly between countries, and a comparison based on the compilation of European
734 forest inventories by Schelhaas et al. (2006) would be challenging without full
735 documentation of each inventory's method. In this case, a possibility for improving the
736 performance of ORCHIDEE-FM for the basal area increment would be to force the model

737 for its initial conditions. If the model were fed with the measured tree circumference
738 distribution before the productivity measurement by surface coring, ORCHIDEE-FM
739 would be more reliable in its simulation of the basal area increment and would,
740 therefore, provide a meaningful comparison with direct measurements.

741 **5 Conclusion**

742 The double aim of this study was to validate ORCHIDEE-FM at the various temporal and
743 spatial scales necessary for a GVM and to separate the modelling error due to the
744 simulation of management from that due to the simulation of productivity. We showed
745 that ORCHIDEE-FM performs reasonably well over long time-scales for most stand-level
746 variables (tree density, basal area, standing volume, average height, and average
747 circumference) and at spatial scales varying from local to continental with several
748 degrees of continuity between measurements. The performance of ORCHIDEE-FM is,
749 however, less satisfying for fine-scale processes such as competition between trees. In
750 terms of error separation, we showed that when initial conditions and management
751 style are controlled, the error from the FMM management component tends to be
752 lower than that of the ORCHIDEE productivity component. However, the volume
753 inventory data shows that both the management and the productivity components
754 need to be calibrated if we want the model to finely reproduce the conditions of a
755 specific region.

756 The validation of ORCHIDEE-FM also paves the way for its improvement. Specific
757 attention should be paid to thinning parameters, either through more empirical studies
758 or through an optimisation framework. The assimilation of initial conditions in the
759 model could also present the possibility of a comparison with the raw measurements of
760 forest inventories rather than the estimated volume and volume increment. Overall,
761 ORCHIDEE-FM is deemed reliable enough to carry out prospective studies on the large-
762 scale impact of management on climate and on the impact of climate change on
763 business-as-usual management. In these applications, ORCHIDEE-FM will provide a
764 useful complement to inventory-based studies because it allows the separation of the
765 effects of CO₂, climate, and management on wood stocks and wood production.

766 **6 Acknowledgements**

767 We want to acknowledge the contribution of Antoine Colin (IFN), Daniel Rittié (INRA-
768 LERFoB), and Maurizio Teobaldelli (JRC), without whom the work on the datasets that
769 they manage would have been both impossible and meaningless. We also want to thank
770 Eric Dufrêne (CNRS-ESE) and Soenke Zaehle (MPI) for their useful suggestions on the
771 model structure.

772 This work was funded by the French Ministry for Research. It benefited from data
773 generated by the CarboEurope-IP project. This study contributes to the French ANR
774 AUTREMENT project (ANR-06-PADD-002).

775 **7 References**

- 776 Abramowitz, G., Leuning, R., Clark, M. and Pitman, A., 2008. Evaluating the
777 Performance of Land Surface Models. *Journal of Climate*, 21:5468-5481.
- 778 Amiro, B.D., Orchansky, A.L., Barr, A.G., Black, T.A., Chambers, S.D., Chapin, F.S.,
779 Goulden, M.L., Litvak, M., Liu, H.P., McCaughey, J.H., McMillan, A. and Randerson,
780 J.T., 2006. The effect of post-fire stand age on the boreal forest energy balance.
781 *Agricultural and Forest Meteorology*, 140:41-50.
- 782 Baldocchi, D., Falge, E., Gu, L.H., Olson, R., Hollinger, D., Running, S., Anthoni, P.,
783 Bernhofer, C., Davis, K., Evans, R., Fuentes, J., Goldstein, A., Katul, G., Law, B., Lee,
784 X.H., Malhi, Y., Meyers, T., Munger, W., Oechel, W., U, K.T.P., Pilegaard, K., Schmid,
785 H.P., Valentini, R., Verma, S., Vesala, T., Wilson, K. and Wofsy, S., 2001. FLUXNET:
786 A new tool to study the temporal and spatial variability of ecosystem-scale carbon
787 dioxide, water vapor, and energy flux densities. *Bulletin of the American Meteorological*
788 *Society*, 82:2415-2434.
- 789 Beerling, D.J. and Quick, W.P., 1995. A New Technique for Estimating Rates of
790 Carboxylation and Electron-Transport in Leaves of C-3 Plants for Use in Dynamic
791 Global Vegetation Models. *Global Change Biology*, 1:289-294.
- 792 Bellassen, V., Le Maire, G., Dhote, J.F., Viovy, N. and Ciais, P., this issue. Modeling
793 forest management within a global vegetation model – Part 1: model structure and
794 general behaviour. *Ecological Modelling*.
- 795 Bottcher, H., Freibauer, A., Obersteiner, M. and Schulze, E.D., 2008. Uncertainty
796 analysis of climate change mitigation options in the forestry sector using a generic carbon
797 budget model. *Ecological Modelling*, 213:45-62.
- 798 Carvalhais, N., Reichstein, M., Ciais, P., Collatz, G.J., Mahecha, M., Montagnani, L.,
799 Papale, D., Rambal, S. and Seixas, J., in revision. Identification of Vegetation and Soil
800 Carbon Pools out of Equilibrium in a Process Model via Eddy Covariance and Biometric
801 Constraints. *Global Change Biology*.
- 802 Ciais, P., Schelhaas, M.J., Zaehle, S., Piao, S.L., Cescatti, A., Liski, J., Luysaert, S., Le-
803 Maire, G., Schulze, E.D., Bouriaud, O., Freibauer, A., Valentini, R. and Nabuurs, G.J.,
804 2008. Carbon accumulation in European forests. *Nature Geoscience*, 1:425-429.
- 805 Deleuze, C., Pain, O., Dhote, J.F. and Herve, J.C., 2004. A flexible radial increment
806 model for individual trees in pure even-aged stands. *Annals of Forest Science*, 61:327-
807 335.
- 808 Demarty, J., Chevallier, F., Friend, A.D., Viovy, N., Piao, S. and Ciais, P., 2007.
809 Assimilation of global MODIS leaf area index retrievals within a terrestrial biosphere
810 model. *Geophysical Research Letters*, 34:6.
- 811 Desai, A.R., Moorcroft, P.R., Bolstad, P.V. and Davis, K.J., 2007. Regional carbon fluxes
812 from an observationally constrained dynamic ecosystem model: Impacts of disturbance,
813 CO₂ fertilization, and heterogeneous land cover. *Journal of Geophysical Research-*
814 *Biogeosciences*, 112.
- 815 Dhôte, J.-F. and Hervé, J.-C., 2000. Changements de productivité dans quatre forêts de
816 chênes sessiles depuis 1930 : une approche au niveau du peuplement. *Ann. For. Sci.*,
817 57:651-680.

- 818 Dhôte, J.F., 1999. Compétition entre classes sociales chez le chêne sessile et le hêtre.
819 Revue Forestière Française:309-325.
- 820 Gervois, S., Ciais, P., de Noblet-Ducoudre, N., Brisson, N., Vuichard, N. and Viovy, N.,
821 2008. Carbon and water balance of European croplands throughout the 20th century.
822 Global Biogeochemical Cycles, 22.
- 823 Hurtt, G.C., Moorcroft, P.R., Pacala, S.W. and Levin, S.A., 1998. Terrestrial models and
824 global change: challenges for the future. Global Change Biology, 4:581-590.
- 825 IFN, 2006. Observer la forêt française : mission première de l'IFN. L'IF:12.
- 826 IPCC, 2003. Good Practice Guidance for Land-Use, Land-Use Change and Forestry.
827 Intergovernmental Panel on Climate Change, Kanagawa, Japan, 534 p.
- 828 IPCC, 2007. Climate Change 2007: Synthesis Report. Contribution of Working Groups I,
829 II and III to the Fourth Assessment Report of the Intergovernmental Panel on Climate
830 Change. C.W. Team, R.K. Pachauri and A. Reisinger (eds.), Intergovernmental Panel on
831 Climate Change, Geneva, Switzerland, 104 p.
- 832 JRC, 2009. European Forest Yield Table's database,
833 http://afoludata.jrc.ec.europa.eu/DS_Free/abc_intro.cfm.
- 834 Jung, M., Le Maire, G., Zaehle, S., Luyssaert, S., Vetter, M., Churkina, G., Ciais, P.,
835 Viovy, N. and Reichstein, M., 2007. Assessing the ability of three land ecosystem models
836 to simulate gross carbon uptake of forests from boreal to Mediterranean climate in
837 Europe. Biogeosciences, 4:647-656.
- 838 Kalnay, E., Kanamitsu, M., Kistler, R., Collins, W., Deaven, D., Gandin, L., Iredell, M.,
839 Saha, S., White, G., Woollen, J., Zhu, Y., Chelliah, M., Ebisuzaki, W., Higgins, W.,
840 Janowiak, J., Mo, K.C., Ropelewski, C., Wang, J., Leetmaa, A., Reynolds, R., Jenne, R.
841 and Joseph, D., 1996. The NCEP/NCAR 40-year reanalysis project. Bulletin of the
842 American Meteorological Society, 77:437-471.
- 843 Kattge, J., Knorr, W., Raddatz, T. and Wirth, C., 2009. Quantifying photosynthetic
844 capacity and its relationship to leaf nitrogen content for global-scale terrestrial biosphere
845 models. Global Change Biology, 15:976-991.
- 846 Krinner, G., Viovy, N., de Noblet-Ducoudre, N., Ogee, J., Polcher, J., Friedlingstein, P.,
847 Ciais, P., Sitch, S. and Prentice, I.C., 2005. A dynamic global vegetation model for
848 studies of the coupled atmosphere-biosphere system. Global Biogeochemical Cycles,
849 19:44.
- 850 Lanier, L., 1994. Précis de sylviculture. Ecole Nationale du Génie Rural, des Eaux et des
851 Forêts (ENGREF), Nancy, 477 p.
- 852 Lindner, M., Lucht, W., Bouriaud, O., Green, T. and Janssens, I., 2004. Specific Study on
853 Forest Greenhouse Gas Budget. CarboEurope-GHG, Jena, 62 p.
- 854 Lindner, M., Sievanen, R. and Pretzsch, H., 1997. Improving the simulation of stand
855 structure in a forest gap model. Forest Ecology and Management, 95:183-195.
- 856 Loustau, D., 2004. Rapport final du projet CARBOFOR. INRA, Bordeaux, 138 p.
- 857 Luyssaert, S., Inglisma, I., Jung, M., Richardson, A.D., Reichsteins, M., Papale, D., Piao,
858 S.L., Schulzes, E.D., Wingate, L., Matteucci, G., Aragao, L., Aubinet, M., Beers, C.,
859 Bernhoffer, C., Black, K.G., Bonal, D., Bonnefond, J.M., Chambers, J., Ciais, P., Cook,
860 B., Davis, K.J., Dolman, A.J., Gielen, B., Goulden, M., Grace, J., Granier, A., Grelle, A.,
861 Griffis, T., Grunwald, T., Guidolotti, G., Hanson, P.J., Harding, R., Hollinger, D.Y.,
862 Hutrya, L.R., Kolar, P., Kruijt, B., Kutsch, W., Lagergren, F., Laurila, T., Law, B.E., Le

863 Maire, G., Lindroth, A., Loustau, D., Malhi, Y., Mateus, J., Migliavacca, M., Misson, L.,
864 Montagnani, L., Moncrieff, J., Moors, E., Munger, J.W., Nikinmaa, E., Ollinger, S.V.,
865 Pita, G., Rebmann, C., Rouspard, O., Saigusa, N., Sanz, M.J., Seufert, G., Sierra, C.,
866 Smith, M.L., Tang, J., Valentini, R., Vesala, T. and Janssens, I.A., 2007. CO2 balance of
867 boreal, temperate, and tropical forests derived from a global database. *Global Change*
868 *Biology*, 13:2509-2537.

869 Masek, J.G. and Collatz, G.J., 2006. Estimating forest carbon fluxes in a disturbed
870 southeastern landscape: Integration of remote sensing, forest inventory, and
871 biogeochemical modeling. *Journal of Geophysical Research*, 111:G01006.

872 Meteo-France, 2009. Précipitations annuelles (en mm), période 1961-1990,
873 <http://www.languedoc-roussillon.ecologie.gouv.fr/>.

874 Moorcroft, P.R., Hurtt, G.C. and Pacala, S.W., 2001. A method for scaling vegetation
875 dynamics: The ecosystem demography model (ED). *Ecological Monographs*, 71:557-
876 585.

877 Morales, P., Sykes, M.T., Prentice, I.C., Smith, P., Smith, B., Bugmann, H., Zierl, B.,
878 Friedlingstein, P., Viovy, N., Sabate, S., Sanchez, A., Pla, E., Gracia, C.A., Sitch, S.,
879 Arneeth, A. and Ogee, J., 2005. Comparing and evaluating process-based ecosystem
880 model predictions of carbon and water fluxes in major European forest biomes. *Global*
881 *Change Biology*, 11:2211-2233.

882 Nabuurs, G.J., Hengeveld, G., Heidema, N., Brus, D., Goedhart, P., Walvoort, D., van
883 den Wyngaert, I., van der Werf, B., Tröltzsch, K., Lindner, M., Zanchi, G., Gallaun, H.,
884 Schwaiger, H., Teobaldelli, M., Seufert, G. and Kenter, B., 2008. Mapping the continent:
885 High resolution forest resource analyses of European forests. *The European Carbon*
886 *Balance - Research Highlights 2008*. CarboEurope-IP (eds.), 4 p.

887 Nagy, M.T., Janssens, I.A., Yuste, J.C., Carrara, A. and Ceulemans, R., 2006. Footprint
888 adjusted net ecosystem CO2 exchange and carbon balance components of a temperate
889 forest. *Agricultural and Forest Meteorology*, 139:344-360.

890 Oreskes, N., Shraderfrechette, K. and Belitz, K., 1994. Verification, Validation, and
891 Confirmation of Numerical-Models in the Earth-Sciences. *Science*, 263:641-646.

892 Reichstein, M., Ciais, P., Papale, D., Valentini, R., Running, S., Viovy, N., Cramer, W.,
893 Granier, A., Ogee, J., Allard, V., Aubinet, M., Bernhofer, C., Buchmann, N., Carrara, A.,
894 Grunwald, T., Heimann, M., Heinesch, B., Knohl, A., Kutsch, W., Loustau, D., Manca,
895 G., Matteucci, G., Miglietta, F., Ourcival, J.M., Pilegaard, K., Pumpanen, J., Rambal, S.,
896 Schaphoff, S., Seufert, G., Soussana, J.F., Sanz, M.J., Vesala, T. and Zhao, M., 2007.
897 Reduction of ecosystem productivity and respiration during the European summer 2003
898 climate anomaly: a joint flux tower, remote sensing and modelling analysis. *Global*
899 *Change Biology*, 13:634-651.

900 Reineke, L.H., 1933. Perfecting a stand-density index for even-aged forests. *Journal of*
901 *Agricultural Research*, 46:627-638.

902 Rykiel, E.J., 1996. Testing ecological models: The meaning of validation. *Ecological*
903 *Modelling*, 90:229-244.

904 Santaren, D., 2006. Optimisation des paramètres du modèle de biosphère ORCHIDEE à
905 partir de mesures sur site des flux de carbone, d'eau et d'énergie, Université Versailles
906 Saint-Quentin, Versailles, 190 p.

- 907 Sato, H., Itoh, A. and Kohyama, T., 2007. SEIB-DGVM: A new dynamic global
 908 vegetation model using a spatially explicit individual-based approach. *Ecological*
 909 *Modelling*, 200:279-307.
- 910 Schaefer, K., Collatz, G.J., Tans, P., Denning, A.S., Baker, I., Berry, J., Prihodko, L.,
 911 Suits, N. and Philpott, A., 2008. Combined Simple Biosphere/Carnegie-Ames-Stanford
 912 Approach terrestrial carbon cycle model. *Journal of Geophysical Research-*
 913 *Biogeosciences*, 113:13.
- 914 Schelhaas, M.J., Varis, S., Schuck, A. and Nabuurs, G.J., 2006. EFISCEN Inventory
 915 Database, http://www.efi.int/portal/virtual_library/databases/efiscen/.
- 916 Smith, P., Powlson, D.S., Smith, J.U. and Elliott, E.T., 1997. Special issue - Evaluation
 917 and comparison of soil organic matter models using datasets from seven long-term
 918 experiments - Preface. *Geoderma*, 81:1-3.
- 919 Soares, P., Tome, M., Skovsgaard, J.P. and Vanclay, J.K., 1995. Evaluating a Growth
 920 Model for Forest Management Using Continuous Forest Inventory Data. *Forest Ecology*
 921 *and Management*, 71:251-265.
- 922 Thornton, P.E., Law, B.E., Gholz, H.L., Clark, K.L., Falge, E., Ellsworth, D.S., Golstein,
 923 A.H., Monson, R.K., Hollinger, D., Falk, M., Chen, J. and Sparks, J.P., 2002. Modeling
 924 and measuring the effects of disturbance history and climate on carbon and water budgets
 925 in evergreen needleleaf forests. *Agricultural and Forest Meteorology*, 113:185-222.
- 926 Turner, D.P., Ritts, W.D., Cohen, W.B., Maeirsperger, T.K., Gower, S.T., Kirschbaum,
 927 A.A., Running, S.W., Zhao, M.S., Wofsy, S.C., Dunn, A.L., Law, B.E., Campbell, J.L.,
 928 Oechel, W.C., Kwon, H.J., Meyers, T.P., Small, E.E., Kurc, S.A. and Gamon, J.A., 2005.
 929 Site-level evaluation of satellite-based global terrestrial gross primary production and net
 930 primary production monitoring. *Global Change Biology*, 11:666-684.
- 931 Urbanski, S., Barford, C., Wofsy, S., Kucharik, C., Pyle, E., Budney, J., McKain, K.,
 932 Fitzjarrald, D., Czirkowsky, M. and Munger, J.W., 2007. Factors controlling CO₂
 933 exchange on timescales from hourly to decadal at Harvard Forest. *Journal of Geophysical*
 934 *Research-Biogeosciences*, 112.
- 935 Vacchiano, G., Motta, R., Long, J.N. and Shaw, J.D., 2008. A density management
 936 diagram for Scots pine (*Pinus sylvestris* L.): A tool for assessing the forest's protective
 937 effect. *Forest Ecology and Management*, 255:2542-2554.
- 938 Vetter, M., Churkina, G., Jung, M., Reichstein, M., Zaehle, S., Bondeau, A., Chen, Y.,
 939 Ciais, P., Feser, F., Freibauer, A., Geyer, R., Jones, C., Papale, D., Tenhunen, J.,
 940 Tomelleri, E., Trusilova, K., Viovy, N. and Heimann, M., 2008. Analyzing the causes
 941 and spatial pattern of the European 2003 carbon flux anomaly using seven models.
 942 *Biogeosciences*, 5:561-583.
- 943 Viovy, N., Calvet, J.C., Ciais, P., Dolman, A.J., Gusev, Y., El Mayaar, M., Moors, E.,
 944 Nasanova, O., Pitman, A., Polcher, J., Rivalland, V., Shmakin, A. and Verseghy, D., in
 945 prep. The PILPS-CARBON model evaluation experiment: a test bed for simulating
 946 water, energy and carbon exchange over a forest canopy.
- 947 Wang, X., Fang, J., Tang, Z. and Zhu, B., 2006. Climatic control of primary forest
 948 structure and DBH-height allometry in Northeast China. *Forest Ecology and*
 949 *Management*, 234:264.
- 950 Willmott, C.J., 1982. Some Comments on the Evaluation of Model Performance. *Bulletin*
 951 *of the American Meteorological Society*, 63:1309-1313.

952 Yang, Y. and Titus, S.J., 2002. Maximum size-density relationship for constraining
953 individual tree mortality functions. *Forest Ecology and Management*, 168:259-273.
954 Zaehle, S., Sitch, S., Prentice, I.C., Liski, J., Cramer, W., Erhard, M., Hickler, T. and
955 Smith, B., 2006. The importance of age-related decline in forest NPP for modeling
956 regional carbon balances. *Ecological Applications*, 16:1555-1574.
957
958
959

960 **Tables**

Simulation	Dataset	Model used	Source of woody NPP	Initial conditions	Time period	Validated variables
PP _f	Permanent plots	FMM	Data	Data	First measurement → Last measurement	dens, ba, av _{circ} , circ _{min} , circ _{max} , distrib, σ, γ
PP _c	Permanent plots	ORCHIDEE-FM	Model	Data	First measurement → Last measurement	dens, ba, av _{circ} , circ _{min} , circ _{max} , σ, γ, vol _{tot}
PP _{ic}	Permanent plots	FMM	Data	Model	Year 0 → First measurement	dens, ba, av _{circ} , circ _{min} , circ _{max}
YT _f	Yield tables	FMM	Data	Model	Year 0 → Year 80	dens, ba, dom _{height} , av _{height} , av _{circ} , vol _{main}
NFI _{std}	National Forest Inventory	ORCHIDEE	Model	Model	1876, 1916, 1956 → 2006	NPP _{woody} , vol _{main}
NFI _{fmm}	National Forest Inventory	ORCHIDEE-FM	Model	Model	1876, 1916, 1956 → 2006	NPP _{woody} , vol _{main}
NFI _{opt}	National Forest Inventory	ORCHIDEE-FM, optimized photosynthesis	Model	Model	1876, 1916, 1956 → 2006	NPP _{woody} , vol _{main}
NFI _{st}	National Forest Inventory	ORCHIDEE-FM, self-thinning only	Model	Model	1876, 1916, 1956 → 2006	NPP _{woody} , vol _{main}

961

962 Table 1. Simulations summary

963 Variable abbreviations: dens (tree density), ba (basal area), av_{circ} (average964 circumference), circ_{min} (minimum circumference), circ_{max} (maximum circumference),

965 distrib (circumference distribution), σ (threshold circumference for basal area growth), γ

966 (competition index), vol_{tot} (total wood volume produced), vol_{th} (cumulated thinned967 wood volume), NPP_{woody} (annual wood increment), vol_{main} (standing wood volume).

968

Validation	Variable name	EF	EF _{stat}	AB	AB _{stat}	RMSEs/RMSEu
PP _f vs data						
	dens	0.6	0.40	18%	1%	0.40
	ba	0.56	0.29	2%	10%	0.43
	vol _{main}	0.6	0.39	4%	9%	0.15
	av _{circ}	0.53	0.77	-5%	6%	0.57
	circ _{min}	-0.33	0.36	-25%	46%	1.30
	circ _{max}	0.36	0.67	10%	-3%	0.67
	σ	-0.11	-0.14	16%	72%	0.69
	γ	-0.27	0.01	15%	4%	0.91
PP _{fi} vs data						
	dens	-0.33	-0.29	30%	2%	0.02
	ba	-0.15	-0.90	-12%	13%	0.13
	vol _{main}	0.09	-1.59	-9%	18%	0.18
	av _{circ}	0.09	0.10	-3%	0%	0.10
	circ _{min}	-0.22	0.05	45%	10%	0.30
	circ _{max}	-0.45	-1.24	22%	30%	0.10
PP _c vs PP _f						
	dens	0.16	na	-13%	na	0.72
	ba	0.19	na	1%	na	0.68
	vol _{main}	0.57	na	6%	na	0.77
	vol _{tot}	0.08	na	22%	na	0.85
	av _{circ}	0.21	na	14%	na	0.81
	circ _{min}	0.72	na	10%	na	0.94
	circ _{max}	0.54	na	12%	na	1.09
	σ	0.22	na	10%	na	1.05
	γ	-1.12	na	27%	na	1.00
YT _f vs data						
	dens	-8	-0.08	161%	96%	0.83
	av _{circ}	-0.67	0.48	-18%	-7%	0.78
	ba	0.52	0.41	10%	13%	0.33
	dom _{height}	0.32	0.63	-9%	4%	0.62
	av _{height}	-0.85	0.60	-35%	0%	1.33
	vol _{main}	0.83	0.82	-2%	16%	0.44
	vol _{th}	0.45	0.81	54%	-3%	0.96

969

970 Table 2. Efficiencies and average biases of PP and YT simulations

971 Modelling efficiency of ORCHIDEE-FM (EF), modelling efficiency of the relevant

972 statistical model (EF_{stat}), average bias (AB), and systematic/unsystematic error ratio

973 (RMSEs/RMSEu) for three validations.

974 Variable abbreviations: dens (tree density), ba (basal area), av_{circ} (average975 circumference), circ_{min} (minimum circumference), circ_{max} (maximum circumference),

976 distrib (circumference distribution), σ (threshold circumference for basal area growth), γ

977 (competition index), vol_{tot} (total wood volume produced), vol_{th} (cumulated thinned
 978 wood volume), $\text{NPP}_{\text{woody}}$ (annual wood increment), vol_{main} (standing wood volume).
 979

Variable	ES_{fmm} (%)
dens	32%
ba	35%
vol_{main}	48%
av_{circ}	37%
circ_{min}	83%
circ_{max}	58%
σ	59%
γ	37%

980

981 Table 3. The FMM share of the total modelling error based on the permanent plots
 982 dataset (ES_{fmm})

983 For the definition of ES_{fmm} , see Eq. 11.

984 Variable abbreviations: dens (tree density), ba (basal area), vol_{main} (standing wood
 985 volume), av_{circ} (average circumference), circ_{min} (minimum circumference), circ_{max}
 986 (maximum circumference), σ (threshold circumference for basal area growth), γ
 987 (competition index).

988

Region (label of Figure 9d)	Broadleaves				Needleleaves			
	Volume increment (m ³ .ha ⁻¹ .yr ⁻¹)		Relative difference to national average		Volume increment (m ³ .ha ⁻¹ .yr ⁻¹)		Relative difference to national average	
	Measured	Simulated	Measured	Simulated	Measured	Simulated	Measured	Simulated
Parisian Basin (1)	10.3	8.7	10%	-12%	15.2	6.8	-10%	-26%
Mediterranean (2)	3.8	6.2	-59%	-37%	8.8	9.0	-48%	-2%
Toulouse (3)	7.3	6.6	-21%	-34%	16.1	7.1	-5%	-23%
North-East (4)	12.7	12.0	36%	21%	23.0	11.3	36%	23%
Britanny (5)	9.2	14.2	-2%	44%	17.7	16.0	5%	74%
South-West (6)	10.8	9.0	15%	-9%	12.6	8.8	-26%	-4%
Mid-Atlantic (7)	8.3	8.6	-12%	-13%	12.3	7.3	-27%	-20%
France	9.4	9.9	0%	0%	16.9	9.2	0%	0%

989

990 Table 4. Regional breakdown of the measured and simulated (IFN_{fmm50}) annual volume

991 increment

992 The exact boundaries of these regions are given in Figure 6 of the supplementary

993 materials.

994

Plant functional type	Study	Improved Vc _{max}	Vc _{max} change from standard value
Temperate needleleaves			
	This study (ORCHIDEE model)	41.7	19%
	Kattge et al., 2009 (BETHY)	62.5	116%
Temperate broadleaves			
	This study (ORCHIDEE model)	55.0	0%
	Kattge et al., 2009 (BETHY)	57.7	65%

995

996 Table 5. Improved average v_{cmax} values

997

998 **Annexes**

- 999 AB: Average Bias
- 1000 EF: Modelling Efficiency
- 1001 FMM: Forest Management Module
- 1002 GPP: Gross Primary Productivity
- 1003 GVM: Global Vegetation Model
- 1004 HR: Heterotrophic Respiration
- 1005 LAI: Leaf Area Index
- 1006 NEP: Net Ecosystem Productivity
- 1007 NFI: National Forest Inventory
- 1008 NPP: Net Primary Productivity
- 1009 ORCHIDEE-FM: Name of the new version of the ORCHIDEE GVM, which includes a forest
- 1010 management module
- 1011 PFT: Plant Functional Type
- 1012 PP: Permanent Plot
- 1013 YT: Yield Table
- 1014 Annex 1. List of abbreviations
- 1015

ID	Departement	Species	Age at last measurement year	First measurement year	Last measurement year	Post thinning relative density index	Size (ha)
1	Loir-et-Cher	oak	201	1927	2006	0.8	1
2	Allier	oak	153	1931	2003	0.5	1
3	Allier	oak	153	1931	2003	0.8	1
4	Meurthe-et-Moselle	mixed oak/beech	151	1904	2006	0.7	1
5	Meurthe-et-Moselle	oak	122	1959	2007	0.5	0.5
6	Meurthe-et-Moselle	oak	122	1959	2007	0.8	0.5
7	Seine-Maritime	beech	124	1931	2004	0.35	1
8	Seine-Maritime	beech	124	1931	2004	0.5	1
9	Seine-Maritime	beech	124	1931	2004	0.35	1
10	Seine-Maritime	beech	124	1931	2004	0.7	1
11	Orne	oak	165	1934	2005	0.8	1
12	Orne	oak	165	1934	2005	0.5	1
13	Meurthe-et-Moselle	beech	140	1904	1995	0.8	0.2
14	Meurthe-et-Moselle	beech	140	1904	1995	0.5	0.2
15	Meurthe-et-Moselle	beech	142	1904	1997	0.8	0.25
16	Meurthe-et-Moselle	beech	142	1904	1997	0.5	0.25
17	Meurthe-et-Moselle	beech	151	1904	2006	1	0.25
18	Aisne	beech	118	1922	1978	0.4	0.25
19	Aisne	beech	118	1922	1978	0.8	0.25
20	Aisne	beech	118	1922	1978	1	0.25
21	Aisne	beech	118	1922	1978	0.6	0.5
22	Allier	oak	183	1931	2003	0.7	1
23	Orne	oak	145	1933	2005	0.4	1
24	Meurthe-et-Moselle	beech	151	1904	2006	0.7	0.25
25	Meurthe-et-Moselle	mixed oak/beech	151	1904	2006	0.5	0.25
26	Meurthe-et-Moselle	beech	151	1904	2006	1	0.25
27	Aisne	beech	121	1922	2006	0.5	0.2
28	Aisne	beech	121	1922	2006	0.5	0.2
29	Aisne	beech	121	1922	2006	0.5	0.2
30	Aisne	beech	121	1922	2006	0.5	0.2
31	Vosges	beech	202	1923	1962	0.7	1
32	Meurthe-et-Moselle	oak	137	1928	2007	0.5	1
33	Meurthe-et-Moselle	oak	137	1928	2007	0.8	1
34	Meurthe-et-Moselle	beech	142	1904	1997	0.7	0.25
35	Orne	oak	113	1951	2005	0.8	1
36	Orne	oak	113	1951	2005	0.6	1
37	Orne	oak	113	1951	2005	0.4	1
38	Orne	oak	138	1934	2005	0.8	1
39	Orne	oak	138	1934	2005	0.5	1
40	Orne	oak	200	1934	1960	0.7	2
41	Loir-et-Cher	oak	181	1928	2006	0.8	1
42	Loir-et-Cher	oak	181	1928	2006	0.5	1
43	Loir-et-Cher	oak	146	1928	2006	0.8	1
44	Loir-et-Cher	oak	146	1928	2006	0.5	1
45	Allier	oak	98	1992	2003	0.8	0.5
46	Allier	oak	98	1992	2003	0.5	0.5
47	Aisne	beech	173	1922	1968	0.5	1
48	Aisne	beech	146	1922	2006	0.5	0.53
49	Allier	oak	203	1931	2003	0.7	2
50	Loir-et-Cher	oak	116	1966	2006	0.4	0.83
51	Loir-et-Cher	oak	116	1966	2006	0.4	0.47
52	Loir-et-Cher	oak	116	1966	2006	1	0.47
53	Loir-et-Cher	oak	116	1966	2006	0.8	1
54	Loir-et-Cher	oak	116	1966	2006	0.6	1
55	Orne	oak	188	1934	2005	0.9	1
56	Allier	oak	123	1959	2003	0.9	1
57	Allier	oak	123	1959	2003	0.7	1
58	Allier	oak	123	1959	2003	0.5	1

1016

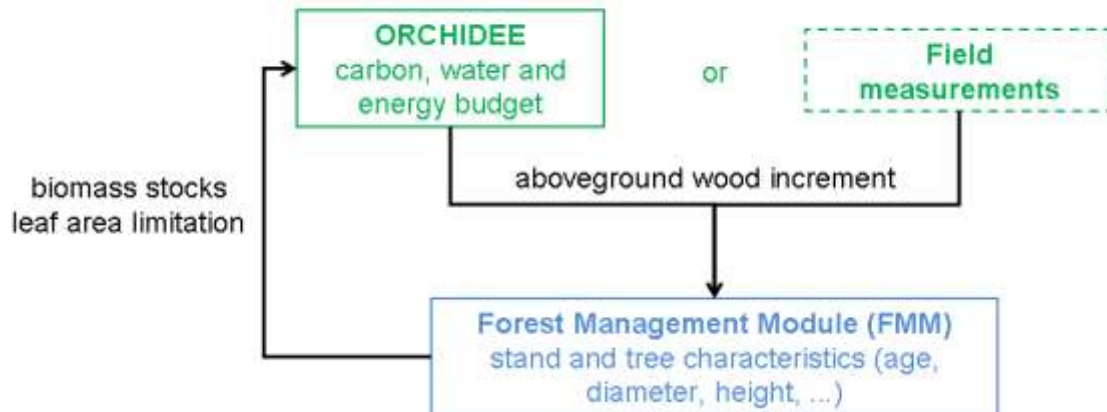
1017 Annex 2. Summary of permanent plot characteristics

1018 Annex 3. Details on the estimation of individual tree growth variables (σ and γ)

1019

1020

1021

1022 **Figure legends**

1023

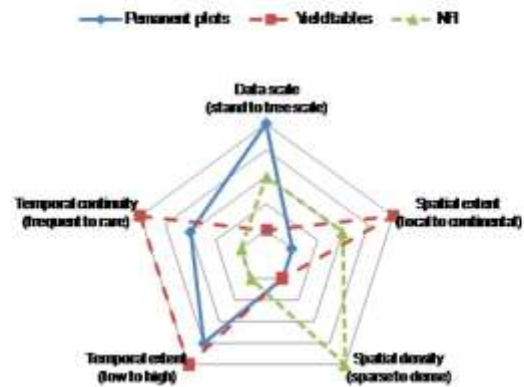
1024 Figure 1. ORCHIDEE-FM: coupled or forced with field measurements

1025 Wood increment can be simulated by the core of ORCHIDEE or derived from site

1026 measurements. The management module simulates its allocation to individual trees in

1027 the stand and computes mortality (self-thinning, anthropogenic thinning or clear-

1028 cutting) based on a density index.



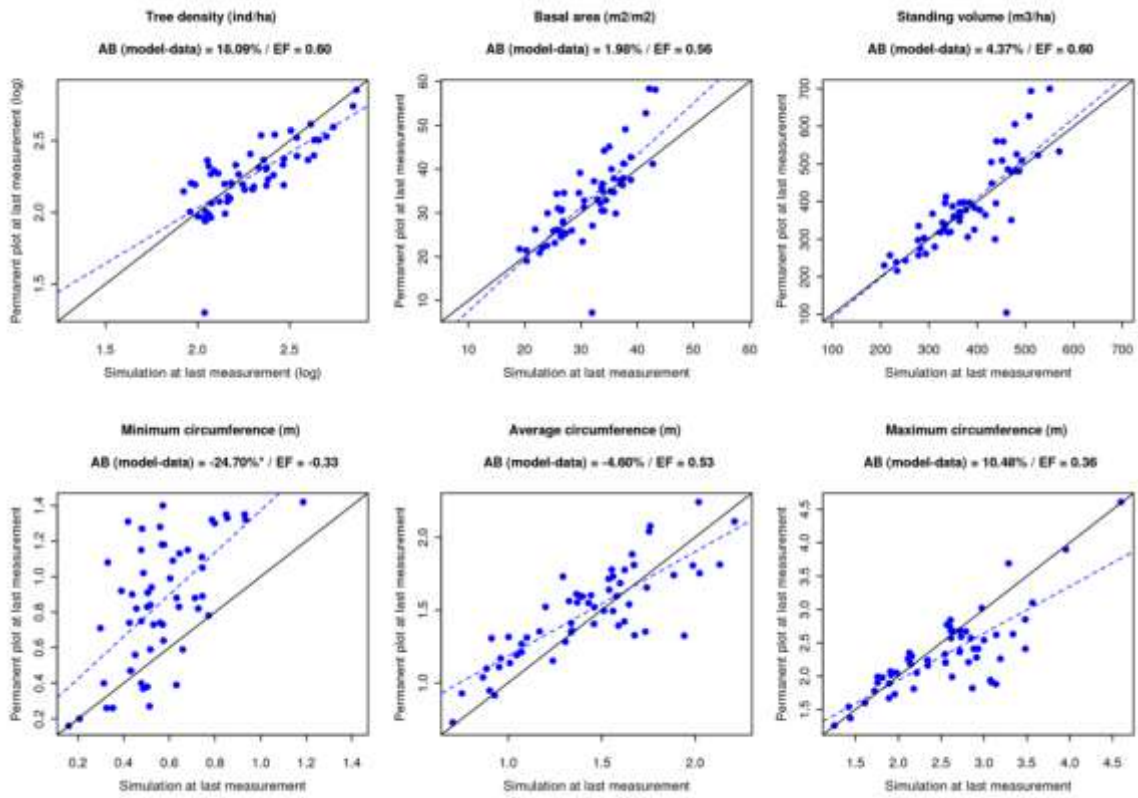
1029

1030 Figure 2. Characteristics of the three datasets used

1031 Eight French forests containing 1 to 10 permanent plots with broadleaves, amounting to

1032 58 plots over the metropolitan territory.

1033



1034

1035 Figure 3. Validation of stand characteristics: PP_f simulation

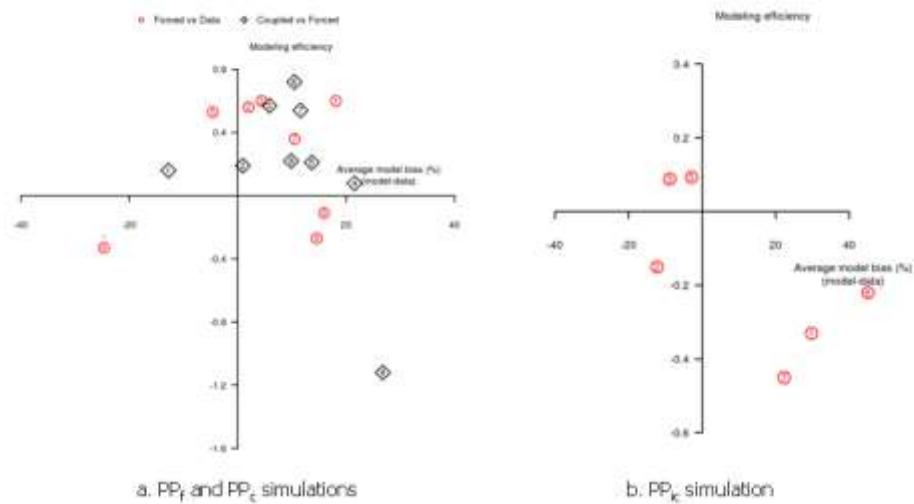
1036 Each blue dot corresponds the state of one permanent plot at its last measurement. The

1037 dotted blue line represents their linear regression. AB and EF are average relative bias

1038 and model efficiency, respectively. An “*” indicates that the systematic error is higher

1039 than the unsystematic error ($RMSEs > RMSEu$).

1040



1041

1042 Figure 4. Summary diagrams of model performance for PP simulations

1043 These diagrams represent model efficiency and average bias for a selected set of stand

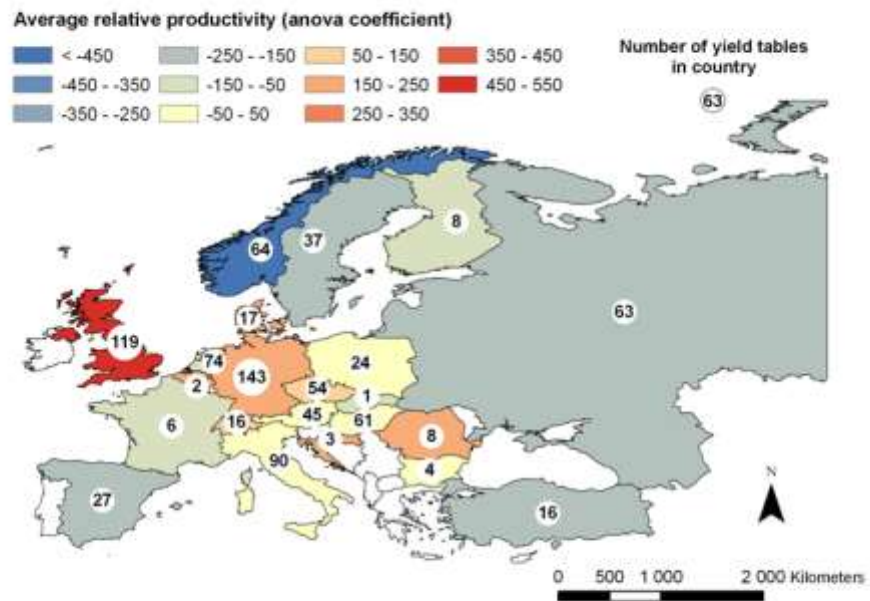
1044 variables. Red circles indicate the ability of the FMM forced with the local wood

1045 increment to reproduce data (PP_f vs. data and PP_{fi} vs. data), whereas black diamonds

1046 indicate the ability of the FMM coupled with the wood increment from ORCHIDEE to
 1047 reproduce the “forced” simulation (PP_c vs. PP_f). An “*” indicates that the systematic
 1048 error is higher than the unsystematic error ($RMSE_s > RMSE_u$).

1049 1. tree density / 2. basal area / 3. standing volume / 4. total volume / 5. average
 1050 circumference / 6. minimum circumference / 7. maximum circumference / 8. sigma / 9.
 1051 gamma

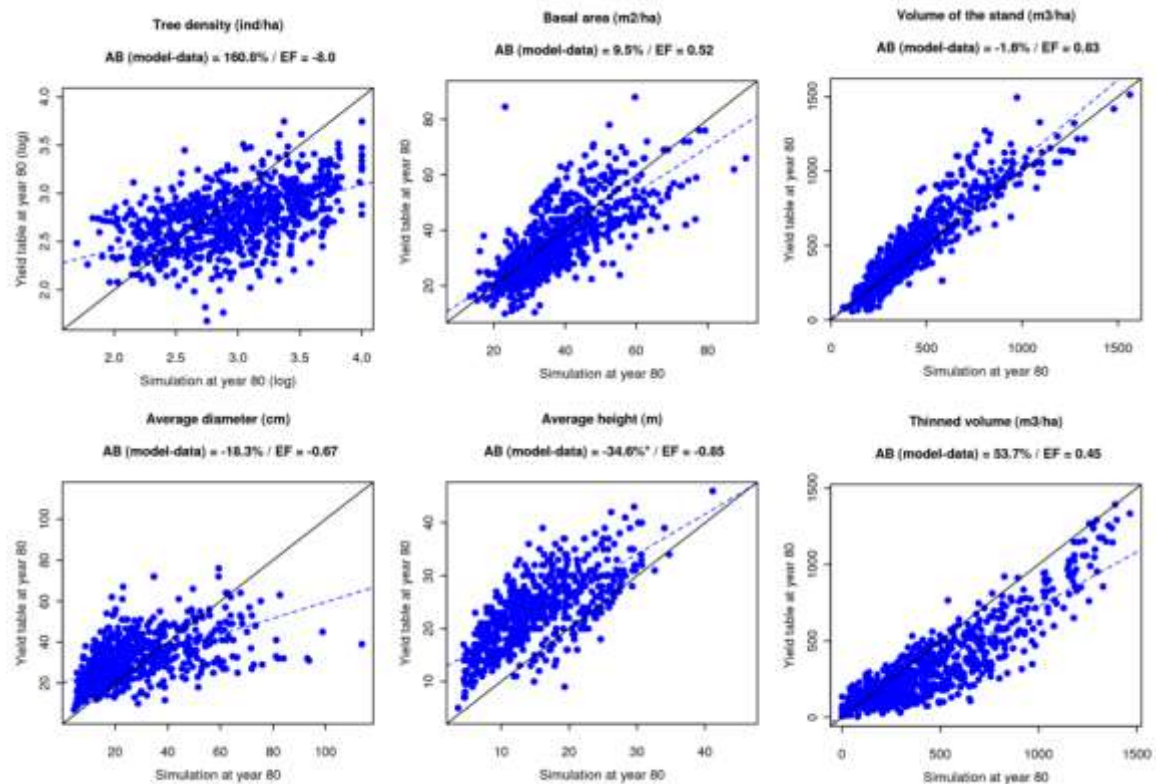
1052



1053

1054 Figure 5. Country productivity index based on the European yield table dataset

1055 The “average relative productivity” index corresponds to the country-specific coefficient
 1056 of the linear mixed model of Equation 4. The studied variable is the volume increment at
 1057 the age of 80, and the two explanatory variables are country and plant functional type.
 1058

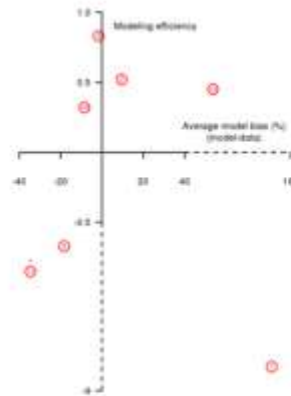


1059

1060 Figure 6. Validation of stand characteristics: Y_{Tf} simulation

1061 Each blue dot corresponds the state of one permanent plot at its last measurement. The
 1062 dotted blue line represents their linear regression. *AB* and *EF* are the average relative
 1063 bias and model efficiency, respectively. An “*” indicates that the systematic error is
 1064 higher than the unsystematic error ($RMSEs > RMSEu$).

1065



1066

1067 Figure 7. Summary diagrams of model performance for the YT_f simulation

1068 This diagram represents the model efficiency and average bias for a selected set of

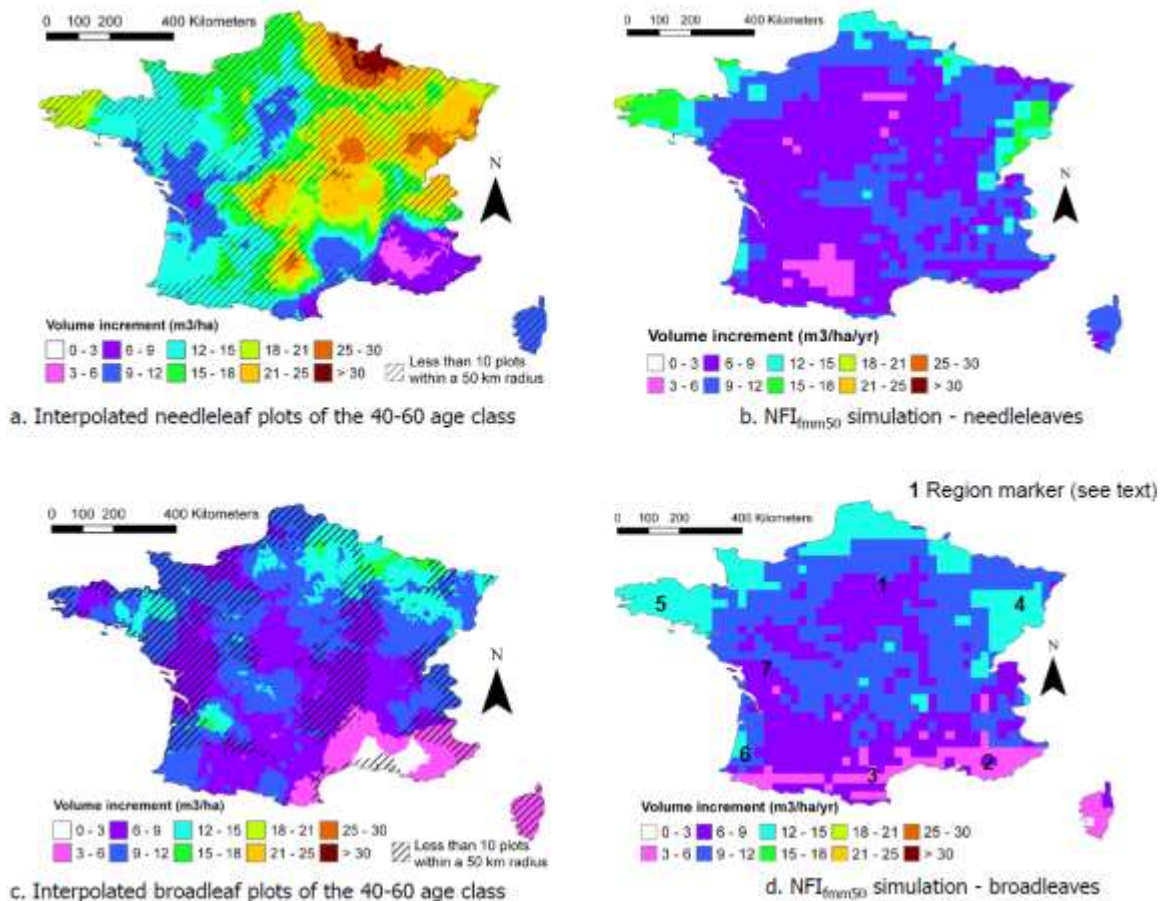
1069 stand variables. An “*” indicates that the systematic error is higher than the

1070 unsystematic error ($RMSE_s > RMSE_u$).

1071 1. tree density / 2. basal area / 3. standing volume / 5. average circumference / 10.

1072 dominant height / 11. average height / 12. thinned volume

1073



1074

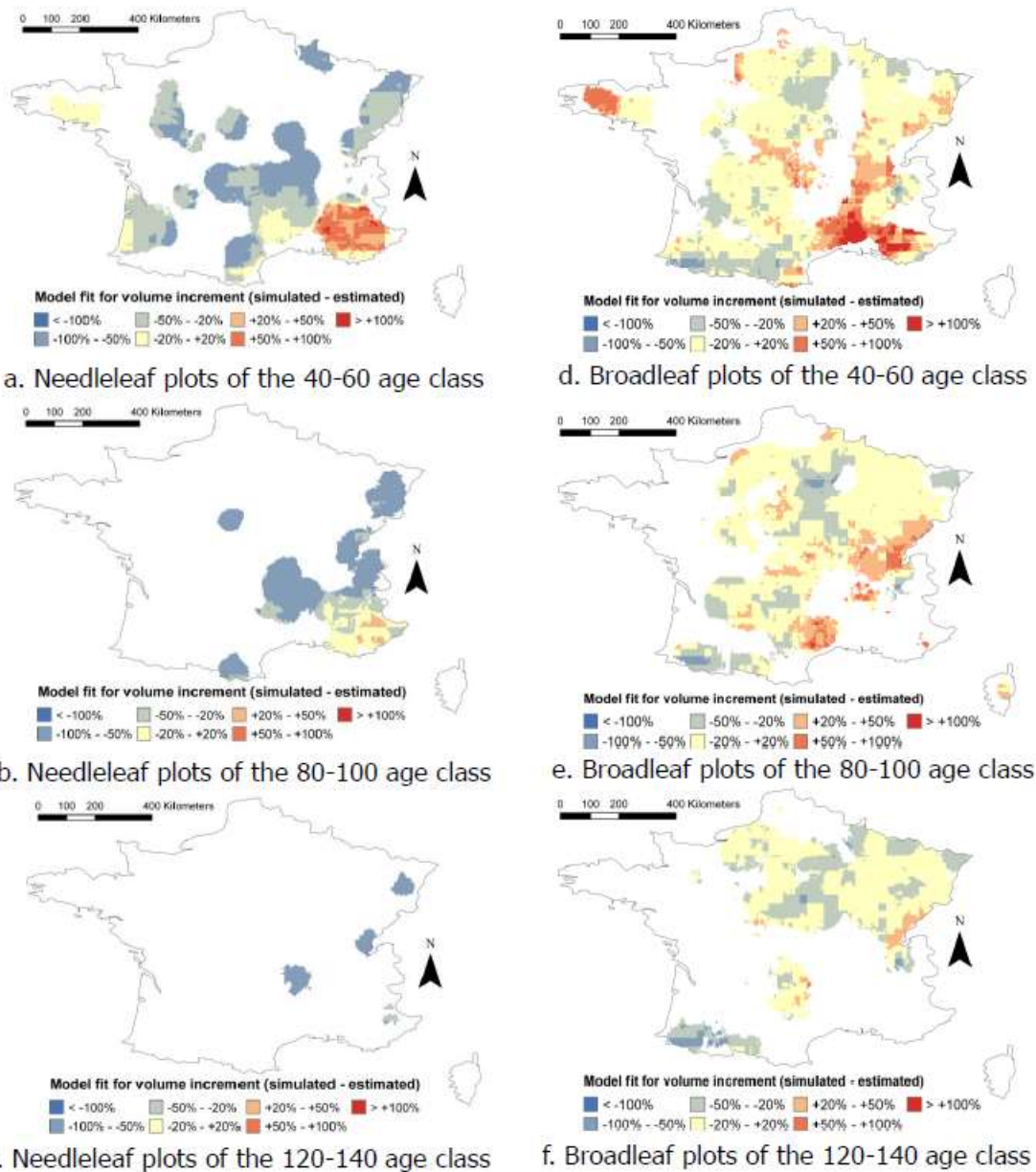
1075 Figure 8. Validation of the volume increment at a regional scale

1076 "Interpolated data" maps (a and c) are derived from National Forest Inventory plots, and

1077 " NFI_{fm50} simulation" maps (b and d) represent the output of ORCHIDEE-FM simulations

1078 for 50-year-old stands.

1079



1080

1081

Figure 9. Model fit for the volume increment: evolution with age

1082

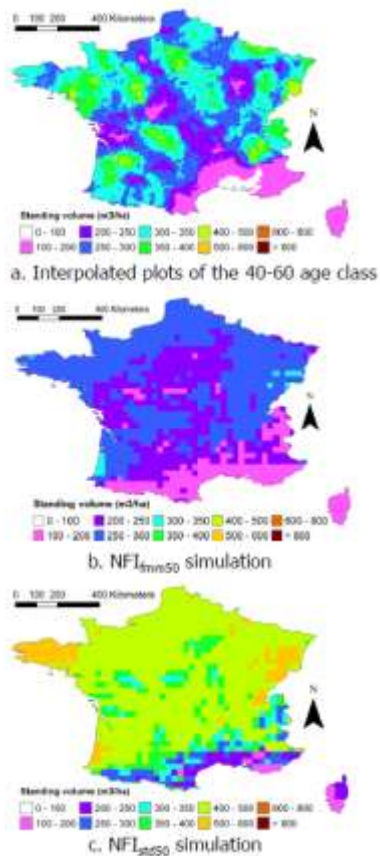
These 6 maps represent the model fit $\left(\frac{NFI_{fmm} - data}{data} \right)$ for the volume increment for

1083

three age classes of needleleaves (a, b, c) and broadleaves (d, e, f). White areas

1084 represent less than 10 data plots within a 55-km radius. Thus, the interpolation is
 1085 considered too weak to assess model fit.

1086

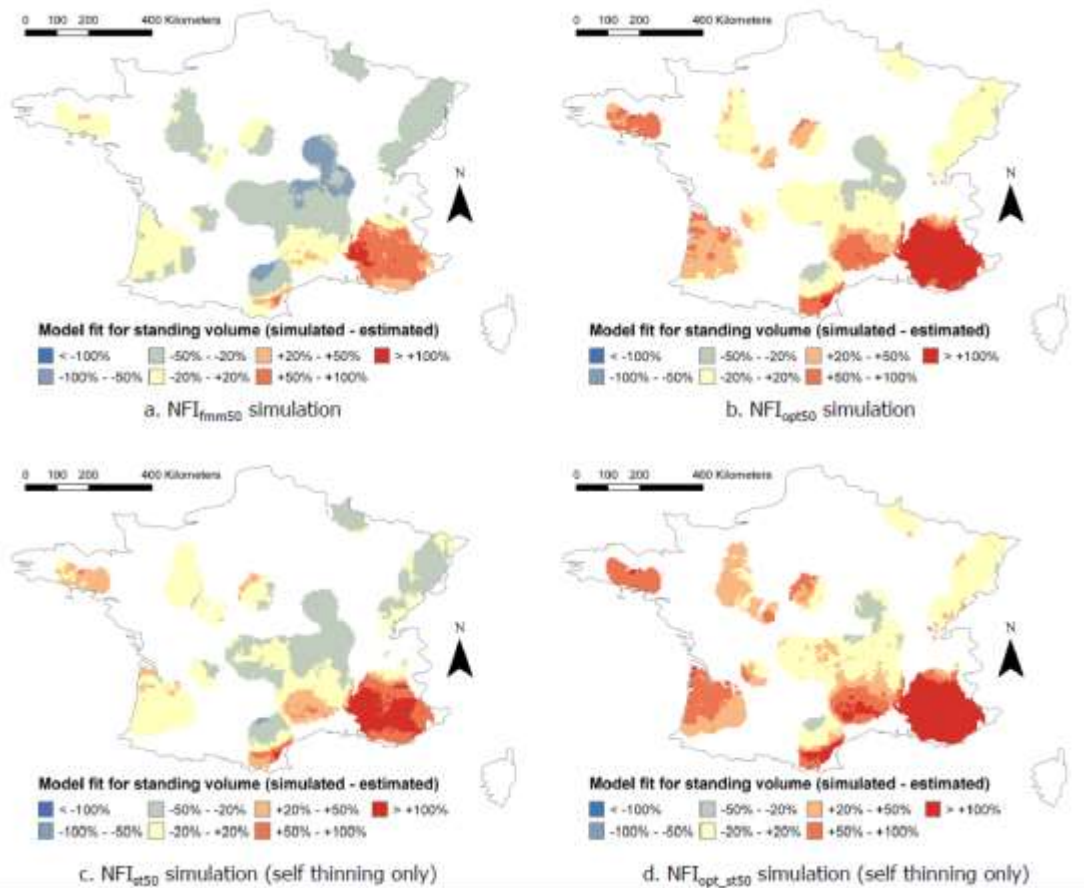


1087

1088 Figure 10. Standing volume of 50-year-old broadleaf stands

1089 The “interpolated data” map (a) is derived from National Forest Inventory broadleaf
 1090 plots of the 40-60-year age class and the “ NFI_{fm50} and NFI_{std50} simulation” maps (b and
 1091 c) represent the output of ORCHIDEE-FM and ORCHIDEE simulations for 50-year-old
 1092 broadleaf stands.

1093



1094

1095 Figure 11. Model fit for standing volume of 50-year-old needleleaf stands

1096 These four maps represent the model fit $\left(\frac{NFI_{fmm} - data}{data}\right)$ for standing volume for four

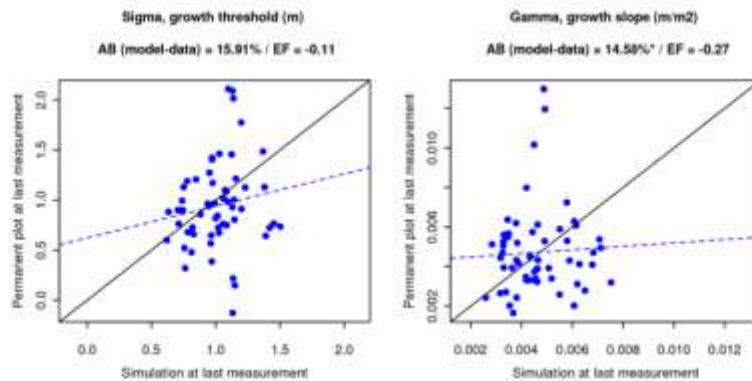
1097 different simulation options: ORCHIDEE-FM (a), ORCHIDEE-FM with optimised

1098 photosynthesis efficiency (b), ORCHIDEE-FM without anthropogenic thinning (c) and

1099 ORCHIDEE-FM both with optimised photosynthesis efficiency and without

1100 anthropogenic thinning (d). White areas represent less than 10 data plots within a 55-

1101 km radius, and the interpolation is, therefore, considered too weak to assess model fit.



1102

1103 Figure 12. Validation of individual tree growth variables (σ and γ): PP_f simulation

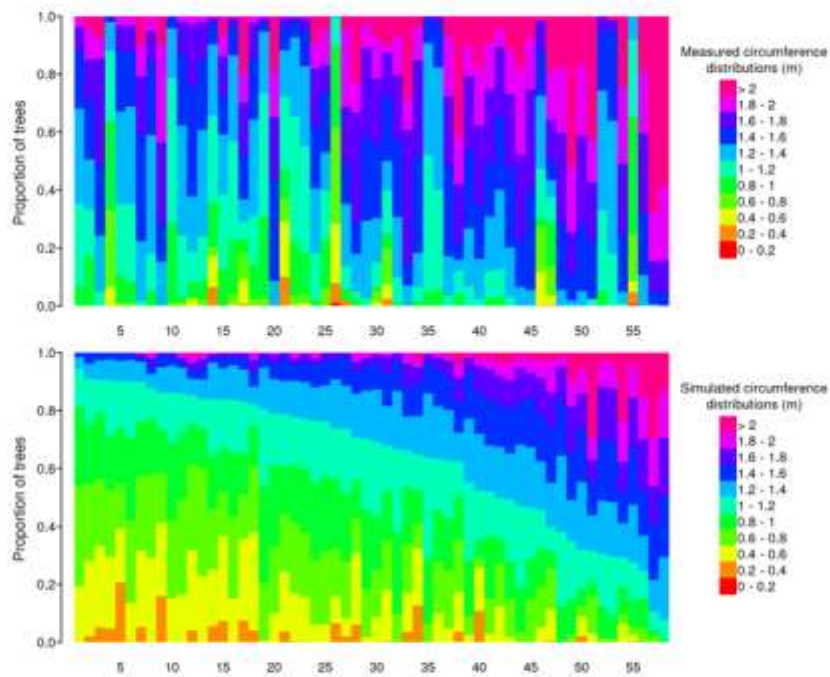
1104 Each blue dot corresponds to the state of one permanent plot at its last measurement.

1105 The dotted blue line represents their linear regression. AB and EF are average relative

1106 bias and model efficiency, respectively. An "*" indicates that the systematic error is

1107 higher than the unsystematic error ($RMSE_s > RMSE_u$).

1108



1109

1110 Figure 13. Validation of circumference distribution: *PPf* simulation

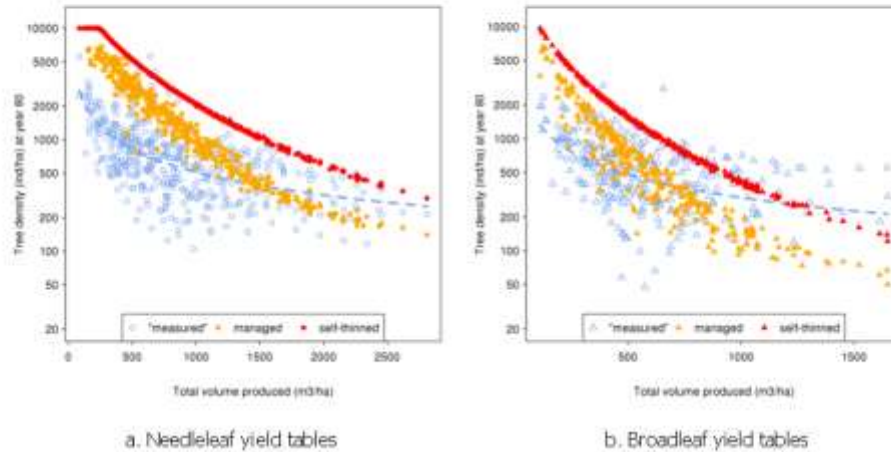
1111 The different hues indicate the repartition of trees between 11 circumference classes

1112 (ordinates) for the last measurement of each permanent plot (abscissa). Permanent

1113 plots were sorted by increasing the simulated proportion of trees in the greater than

1114 1.4-m category.

1115



1116

1117 Figure 14. Self-thinning curves based on yield tables

1118 Full dots represent values of tree density against the total volume produced from the

1119 YT_f simulation (orange for a “managed” scenario and red for a “self-thinning only”

1120 scenario). Empty blue dots represent the corresponding data from yield tables, with a

1121 dashed line for the log-log linear regression.